EUROPEAN ORGANIZATION FOR NUCLEAR RESEARCH

CERN-EP/99-143
October 11, 1999

Tests of the Standard Model‡

Joachim Mnich

CERN EP, 1211 Geneva 23, Switzerland
E-mail: Joachim.Mnich@cern.ch

Abstract

This article describes the status of experimental tests of the Standard Model of Electroweak Interactions. Updated precision measurements from $\mathrm{e^+e^-}$-annihilation at the Z resonance are discussed as well as new results obtained above the Z pole. Significant progress on the determination of the properties of the W boson is achieved by $\mathrm{e^+e^-}$- and $\mathrm{p\bar{p}}$-experiments. A combined analysis of precision electroweak measurements in the framework of the Standard Model leads to an estimate and an upper limit for the mass of the Higgs boson.

1. Introduction

For one decade precision tests of the Standard Model of Electroweak Interactions (SM) [1] in $\mathrm{e^+e^-}$-collisions have been performed by the experiments at the LEP and SLC colliders. The properties of the Z boson, its mass, total and partial decay widths as well as the couplings to fermions, have been measured to very high accuracy. These measurements are sensitive to higher order electroweak radiative corrections and enable tests of the theory beyond the tree level. Now the experiments at the Z resonance are completed and the careful analyses are close to the final stage.

The LEP collider continues the experimental program providing $\mathrm{e^+e^-}$-collisions up to centre-of-mass (cms) energies of 200 GeV and above. At these energies the photon and the Z contribute in an equal manner to the production of fermion pairs allowing the test of electroweak unification. All gauge bosons of the SM are produced in pairs permitting studies of their self-couplings, some of which are predicted by the non-abelian gauge structure of the model. An important measurement is the precise determination of the W boson mass which confronted to the measurements at the Z resonance consists a crucial test of the SM.

‡ *Plenary talk given at the International Europhysics Conference on High Energy Physics 99 Tampere, Finland, 15-21 July 1999*

The tests of the SM in $\mathrm{e^+e^-}$-annihilations are complemented by the experiments performed at the Tevatron $\mathrm{p\bar{p}}$-collider. Most importantly, the discovery of the top quark and the measurements of the top quark and W boson masses contribute to the experimental verification of the theory.

The precision of these measurements is such that they are sensitive to higher order electroweak corrections. Comparing the direct mass measurements of the W boson and the top quark with values derived from the measurements of electroweak couplings and higher order weak corrections allows to verify the SM beyond the tree level. The observed consistency provides great confidence into the validity of the SM and encourages the use of all experimental data to predict the mass of the last unobserved particle of the model: the Higgs boson.

This article is organized as follows: Section 2 reviews the current status of precision measurements at the Z resonance from LEP and SLD. The production of fermion pairs in $\mathrm{e^+e^-}$-collisions above the Z resonance studied at LEP is described in section 3. Studies of the production of neutral bosons, the photon and the Z, are presented in section 4 resulting in limits on hypothetical self-couplings. Significant improvements on the determinations of the properties of the W boson were made recently which are discussed in section 5. Precision electroweak measurements are used in fits in the SM framework to test the model at the level of weak radiative corrections and to estimate the mass of the

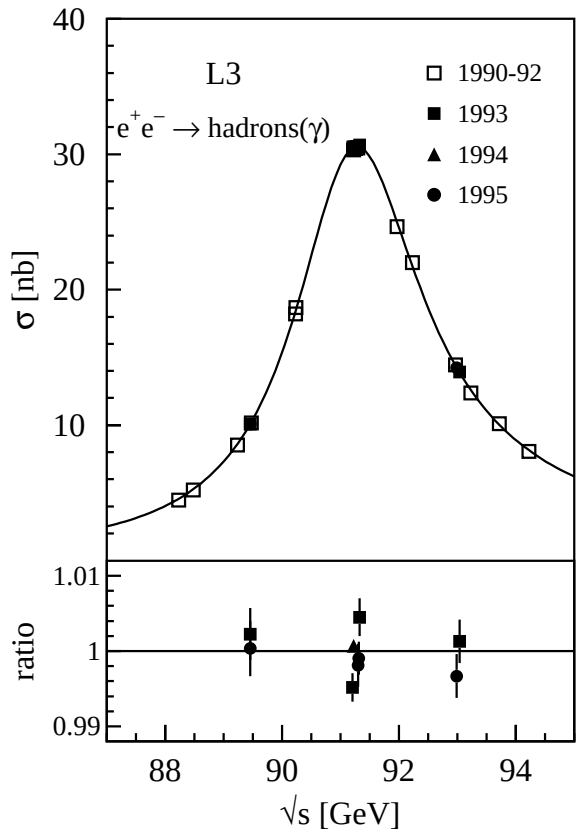

Figure 1. The cross section $e^+e^- \to$ hadrons as function of the cms energy at the Z resonance measured by L3. The solid line shows the result of the fit. At the bottom the ratio of the measured cross sections and the fit result for the data collected in $1993-95$ is shown.

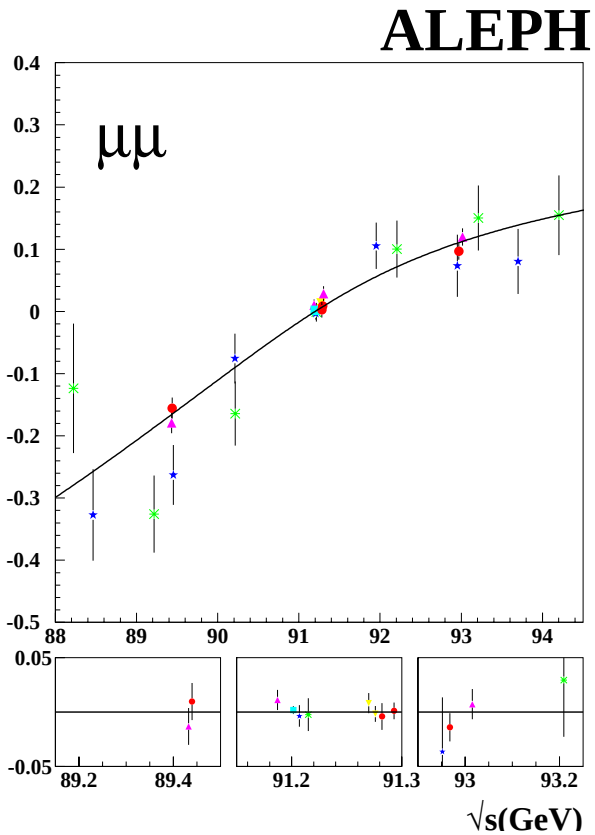

Figure 2. The forward-backward asymmetry in $e^+e^- \to \mu^+\mu^-$ as function of the cms energy at the Z resonance measured by ALEPH. The solid line shows the result of the fit. At the bottom the difference of the measured asymmetry and the fit result is shown.

Higgs boson (section 6). The conclusions and prospects for the future are given in section 7.

Almost all results discussed here are preliminary and reflect the status of the analyses at the time of the conference. As compared to the oral presentation several updated results presented during the meeting are incorporated.

2. Measurements at the Z resonance

2.1. The lineshape of the Z boson

Between 1989 and 1995 the LEP experiments have performed precision measurements at the Z resonance of total cross sections and leptonic forward-backward asymmetries of the reactions:

$$\begin{aligned} e^+e^- \to \text{hadrons}\,, \qquad & e^+e^- \to e^+e^-\,, \\ e^+e^- \to \mu^+\mu^-\,, \qquad & e^+e^- \to \tau^+\tau^-\,. \end{aligned} \tag{1}$$

In total about 17 million Z decays have been observed by the four experiments allowing measurements at the permille level. Two examples of these measurements, the hadronic cross section and muon forward-backward asymmetry, are shown in Figs. 1 and 2. The data are compared to the results of fits performed to extract the Z parameters. The analyses of the four LEP experiments are now close to the final stage [2–4] and their publications are expected in short time.

In order to extract electroweak parameters from these and other measurements, precise theoretical calculations are as important as the experiments themselves. Two programs are used by the LEP collaborations to calculate cross sections, asymmetries and other electroweak observables: ZFITTER [5] and TOPAZ0 [6]. The contributions from t-channel boson exchange and the s-t interference in $e^+e^- \to e^+e^-$ are calculated using ALIBABA [7]. ZFITTER and TOPAZ0 contain calculations of initial state radiation up to $\mathcal{O}(\alpha^3)$ [8], electroweak two-loop corrections

$\mathcal{O}(G_F^2 m_t^4)$ and $\mathcal{O}(G_F^2 m_t^2 m_Z^2)$ [9], QCD final state radiation $\mathcal{O}(\alpha_s^3)$ [10] as well as non-factorizable mixed QCD-electroweak corrections [11]. Cross sections calculated with the two implementations agree at the 10^{-4} level [12, 13].

The remaining theoretical uncertainties on Z parameters are small compared to the experimental precision. Most important are uncertainties on QED corrections, mainly due to pair production by initial state radiation†, which contribute by ± 0.3 MeV, ± 0.5 MeV and $2 \cdot 10^{-4}$ to the errors on the mass m_Z, the total width Γ_Z and the pole cross sections, respectively. There is an additional theoretical uncertainty of ± 0.3 MeV on m_Z from the γZ interference term, which depends on the Higgs boson mass m_H and the QED coupling constant α, and from observed differences in the result when determining m_Z as free parameter of a Breit-Wigner curve or from a fit in the SM framework [15] imposing relations between m_Z and the other parameters of the resonance curve.

An important improvement is the reduction of the theoretical error to $0.6 \cdot 10^{-3}$ [16] on the cross section of low angle Bhabha scattering. This reaction is used by the LEP experiments to determine the luminosity.

From their measurements of total cross sections and forward-backward asymmetries the experiments determine nine parameters: the mass and total width of the Z, the hadronic pole cross section, $\sigma^0_{\rm had}$, and for the three charged leptons the ratios of hadronic to leptonic widths, R_ℓ, and the pole asymmetries, $A^{0,\ell}_{\rm FB}$:

$$\sigma^0_{\rm had} = \frac{12\pi}{m_Z^2}\frac{\Gamma_e\Gamma_{\rm had}}{\Gamma_Z^2}, \quad R_\ell = \frac{\Gamma_{\rm had}}{\Gamma_\ell},$$
$$A^{0,\ell}_{\rm FB} = \frac{3}{4}A_e A_\ell, \quad A_\ell = \frac{2\bar{g}^\ell_V \bar{g}^\ell_A}{(\bar{g}^\ell_V)^2 + (\bar{g}^\ell_A)^2}. \qquad (2)$$

The polarization parameter A_ℓ is given by the effective vector- and axial-vector coupling constants, $\bar{g}^\ell_V$ and $\bar{g}^\ell_A$ [17].

The combination of the experiments is performed on this set of parameters yielding the result shown in Tab. 1. There are small correlations between the parameters [18]. The theoretical errors as discussed above are included. The LEP energy calibration [19] contributes by 1.7 MeV and 1.3 MeV to the errors on m_Z and Γ_Z, and to a lesser extent to the other parameters [15].

Fig. 3 compares the contours in the $A^{0,\ell}_{\rm FB} - R_\ell$ plane for the three lepton species. The three contours agree and assuming lepton universality yields‡:

$$R_\ell = 20.768 \pm 0.024,$$

† Meanwhile additional calculations of initial state pair production have been performed [14] and implemented in updated versions of ZFITTER and TOPAZ0.

‡ For this average as well as in Fig. 3 the tau measurements are corrected for the non-negligible effect of the tau mass.

m_Z	$91\,187.2 \pm 2.1$ MeV
Γ_Z	$2\,499.4 \pm 2.4$ MeV
$\sigma^0_{\rm had}$	41.544 ± 0.037 nb
R_e	20.803 ± 0.049
R_μ	20.786 ± 0.033
R_τ	20.764 ± 0.045
$A^{0,e}_{\rm FB}$	0.0145 ± 0.0024
$A^{0,\mu}_{\rm FB}$	0.0167 ± 0.0013
$A^{0,\tau}_{\rm FB}$	0.0188 ± 0.0017

Table 1. Combined result of the fits to nine parameter (Eq. 2) of the four LEP experiments.

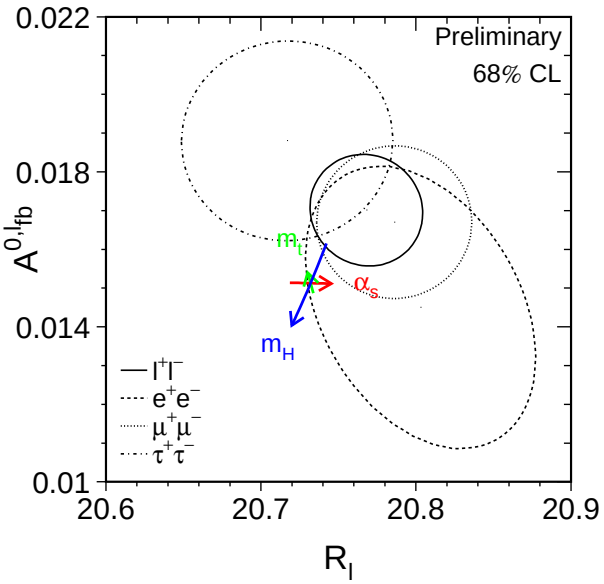

Figure 3. Contours in the $A^{0,\ell}_{\rm FB}$-R_ℓ plane for the three charged leptons obtained from the combination of the four LEP experiments. The solid line shows the result assuming lepton universality. The SM expectation is represented by arrows indicating the dependence on the Higgs mass m_H, the top mass m_t and the strong coupling constant.

$$A^{0,\ell}_{\rm FB} = 0.01701 \pm 0.00095. \qquad (3)$$

The measurements are in agreement with the SM expectation for a light Higgs boson§.

From a parameter transformation the decay widths of the Z boson into hadrons, charged leptons and

§ Throughout this article SM predictions are calculated for 95 GeV $\leq m_H \leq$ 1 TeV, $\alpha_s = 0.119 \pm 0.002$ and using for m_Z, m_t and the QED coupling constant the values and errors listed in Fig. 51.

invisible particles are derived to be:

$$\begin{aligned}\Gamma_{\rm had} &= 1743.9 \pm 2.0 \ {\rm MeV}\,,\\ \Gamma_\ell &= 83.959 \pm 0.089 \ {\rm MeV}\,,\\ \Gamma_{\rm inv} &= 498.80 \pm 1.5 \ {\rm MeV}\,. \end{aligned} \quad (4)$$

These numbers are interpreted in a determination of the number of neutrino families:

$$N_\nu = \frac{\Gamma_{\rm inv}}{\Gamma_\ell}\left(\frac{\Gamma_\ell}{\Gamma_\nu}\right)^{\rm SM} = 2.9835 \pm 0.0083\,. \quad (5)$$

This result is by two standard deviations short of the three known neutrino species. This deficit is mainly caused by the measurement of the hadronic pole cross section which compared to last year [18, 20] increased due to experimental updates and the inclusion of $\mathcal{O}(\alpha^3)$ corrections. Also, the error has improved considerably because of the reduced theoretical uncertainty on the luminosity determination. Assuming three SM neutrino families an upper 95% CL limit on the Z decay width into other, non-standard invisible particles of $\Delta\Gamma_{\rm inv} < 2.0$ MeV is derived.

2.2. Couplings of the Z to charged leptons

Very important contributions to the precise determination of effective couplings of leptons and quarks to the Z boson are provided by the SLD experiment at the SLC $\rm e^+e^-$-collider which has the unique feature of a high degree of polarization of the electron beam. From the relative difference of total cross sections at the Z for left- and right-polarized incoming electrons, $A_{\rm LR} = (\sigma_{\rm e_L} - \sigma_{\rm e_R})/(\sigma_{\rm e_L} + \sigma_{\rm e_R}) = A_{\rm e}$, the couplings of the electron can be precisely measured. Between 1989 and 1998 the SLD experiment collected approximately 550 000 $\rm e^+e^- \to$ hadrons events with polarization of about 75% for most of these data. This results in a measurement of $A_{\rm e}$ of [21]:

$$A_{\rm e} = 0.1511 \pm 0.0022\,. \quad (6)$$

Due to helicity conservation at the vertex the couplings of the final state fermions in $\rm e^+e^- \to f\bar{f}$ can be determined from the polar angular distributions observed for different polarizations of the electrons [22], the left-right forward-backward asymmetry. The results obtained for the three lepton species are summarized in Tab. 2 [21].

Combining the measurements of the hadronic left-right asymmetries and the determinations of A_ℓ in the leptonic channels yields the most precise measurement of the effective weak mixing angle:

$$\sin^2\overline{\vartheta}_{\rm W} = \frac{1}{4}\left(1 - \frac{\bar{g}^\ell_{\rm V}}{\bar{g}^\ell_{\rm A}}\right) = 0.23099 \pm 0.00026\,. \quad (7)$$

$A_{\rm e}$	0.1558 ± 0.0064
A_μ	0.137 ± 0.016
A_τ	0.142 ± 0.016
A_ℓ	0.1523 ± 0.0057

Table 2. Measurements by the SLD experiment of the polarization parameter from leptonic left-right forward-backward asymmetries. At the bottom the combined result for the three lepton species is given.

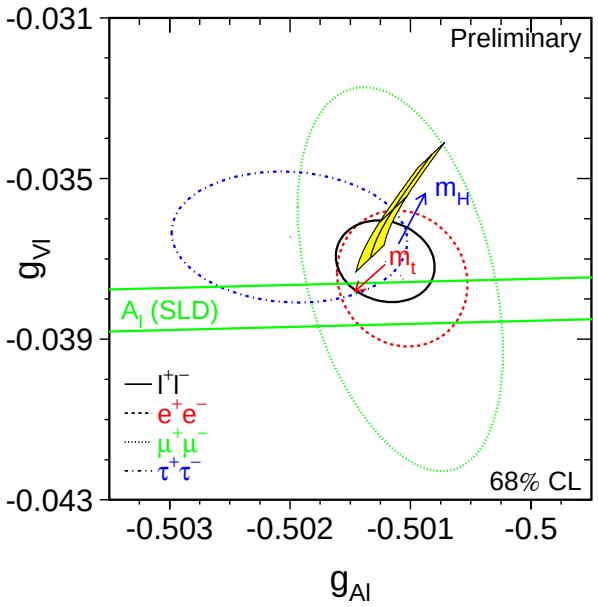

Figure 4. Comparisons of measurements of the effective vector- and axial-vector couplings of the Z to leptons at LEP and SLD. The contours are derived from LEP measurements of the Z lineshape and tau polarization. The solid line represents the combined contour assuming lepton universality. The horizontal band is derived from the SLD measurements of the polarization parameter A_ℓ in $\rm e^+e^- \to$ hadrons and $\rm e^+e^- \to \ell^+\ell^-$. The shaded area corresponds to the SM expectations, with arrows indicating the dependence on the Higgs and top masses.

This result is based on the full data set collected by the SLD experiment.

At LEP, in addition to the measurements described in section 2.1, information on the couplings of the electron and the tau to the Z is obtained from analysing the tau polarization in Z decays. The combined results of the experiments are [21]:

$$A_{\rm e} = 0.1483 \pm 0.0051\,, \quad A_\tau = 0.1425 \pm 0.0044\,. \quad (8)$$

Measurements of the effective coupling constants of the three leptons at LEP are compared in Fig. 4 to the result of SLD and to the SM prediction. The contours

	b-quark	c-quark
$R_{\rm q}$	0.21642 ± 0.00073	0.1674 ± 0.0038
$A_{\rm FB}^{0,{\rm q}}$	0.0988 ± 0.0020	0.0692 ± 0.0037
$A_{\rm q}$	0.911 ± 0.025	0.630 ± 0.026

Table 3. Results of a common fit to measurements of Z decays into b- and c-quarks at LEP and SLD.

	LEP & SLD	SM
A_ℓ	0.1497 ± 0.0016	$0.1431\,^{+0.0054}_{-0.0057}$
$A_{\rm b}$	0.892 ± 0.016	0.935
$A_{\rm c}$	0.625 ± 0.021	0.668

Table 4. Determination of the polarization parameter of b- and c-quarks from measurements at LEP and SLD. The rightmost column contains the SM preditions.

for the three leptons overlap and the combined LEP result agrees with the band representing the combined SLD result (Eq. 7). Again, all measurements are in agreement with the SM for a light Higgs boson mass.

The test of lepton universality in neutral current interactions is quantified by forming ratios of couplings using all measurements:

$$\begin{aligned} \bar{g}_{\rm V}^{\mu}/\bar{g}_{\rm V}^{\rm e} &= 0.946 \pm 0.065\,, \\ \bar{g}_{\rm V}^{\tau}/\bar{g}_{\rm V}^{\rm e} &= 0.955 \pm 0.030\,, \\ \bar{g}_{\rm A}^{\mu}/\bar{g}_{\rm A}^{\rm e} &= 1.0002 \pm 0.0013\,, \\ \bar{g}_{\rm A}^{\tau}/\bar{g}_{\rm A}^{\rm e} &= 1.0019 \pm 0.0015\,. \end{aligned} \tag{9}$$

Imposing lepton universality the effective vector- and axial-vector couplings of charged leptons to the Z are measured at LEP and SLD to be:

$$\begin{aligned} \bar{g}_{\rm V}^{\ell} &= -0.03772 \pm 0.00041\,, \\ \bar{g}_{\rm A}^{\ell} &= -0.50117 \pm 0.00027\,. \end{aligned} \tag{10}$$

2.3. Couplings of the Z to quarks

For b- and c-quarks which can be identified in hadronic Z decays, measurements similar to those for leptonic final state are performed at LEP and SLD: the total cross section, expressed in terms of ratios of partial decay widths to the hadronic width, $R_{\rm q} = \Gamma_{\rm q}/\Gamma_{\rm had}$, forward-backward pole asymmetries and the polarization parameters $A_{\rm q}$ from the left-right forward-backward asymmetry at SLD. The results of the four LEP experiments and SLD are combined in a fit treating correlations between the measurements and the experiments in a coherent way [23, 24]. Tab. 3 presents the result of this combination [25].

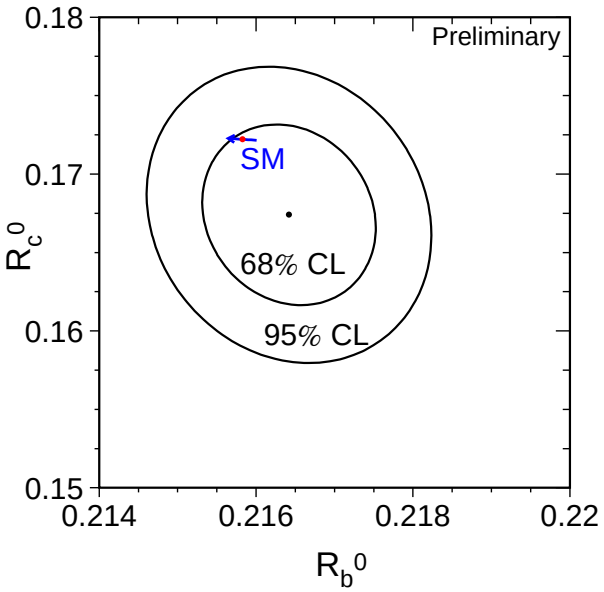

Figure 5. Contours in the $R_{\rm c}$-$R_{\rm b}$ plane obtained from combining the measurements at LEP and SLD. The arrow indicates the SM prediction as a function of the top quark mass.

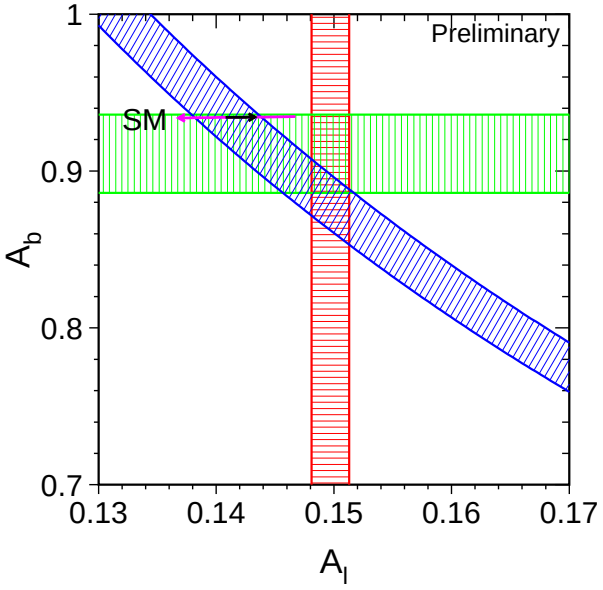

Figure 6. Comparison of the $A_{\rm b}$ measurement of SLD (horizontal band), the combined LEP and SLD result on A_ℓ (vertical) and the b-quark forward-backward asymmetry measured at LEP (sloping).

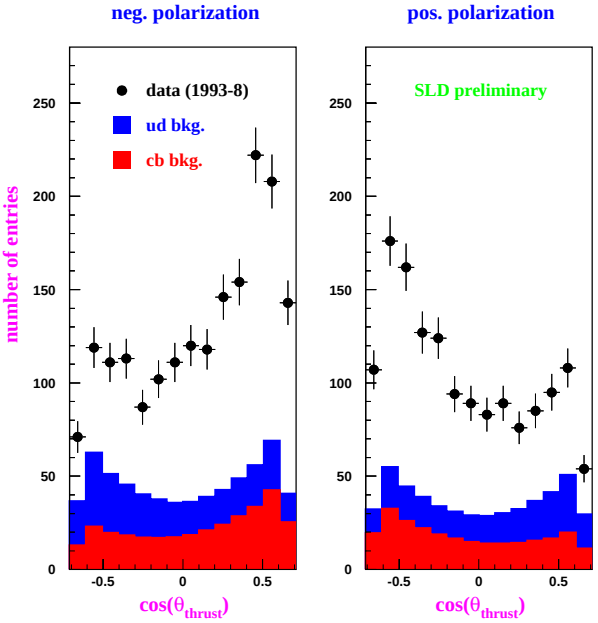

Figure 7. Measured polar angular distributions of $e^+e^- \to s\bar{s}$ events for negative and positive polarization of the incoming electrons.

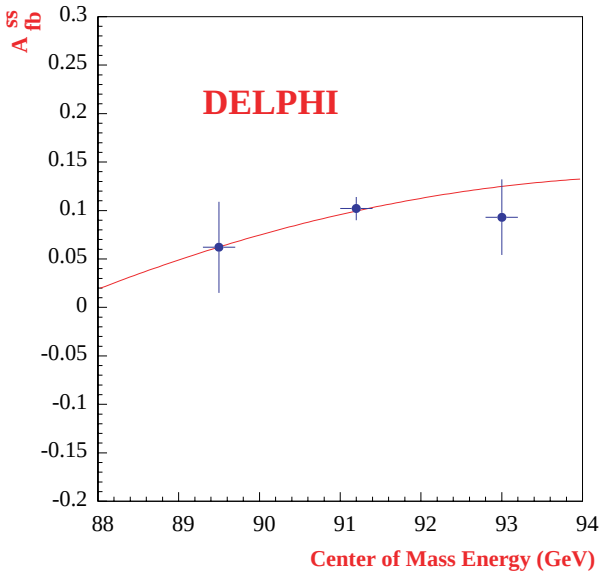

Figure 8. Forward-backward asymmetry in $e^+e^- \to s\bar{s}$ as measured by DELPHI at three cms energies compared to the SM expectation.

The measurements of R_b and R_c are now in good agreement with the SM predictions. This is demonstrated in Fig. 5 which compares contours obtained from the measurements to the SM prediction which falls inside the 68% CL contour.

Fig. 6 compares the measurements of A_b and $A_{FB}^{0,b}$ together with the combined LEP and SLD result of A_ℓ to the SM. All individual measurements agree at the level of one standard deviation with the SM. However, if all measurements are used to derive the polarization parameter of b-quarks it is found to be 2.7 standard deviations away from the expectation. Details are given in Tab. 4. A similar observation, even though less significant, is made for c-quarks. Since these numbers are based on the full statistics of the experiments no significant changes or improvements are expected in near future. Therefore, it will remain unclear if the observed discrepancies are fortuitous accumulations of small deviations in the quantities containing A_b and A_c or if the couplings of the Z to quarks are really different from the SM. It is worth noticing that the partial Z decay width into b-quarks mainly depends on the left-handed coupling whereas A_b is more sensitive to the right-handed.

Now also measurements of strange quark couplings to the Z are available. Identified high momentum K^+, K_s, Λ^0 in hadronic Z decays are used to select $e^+e^- \to s\bar{s}$ events. SLD performed a measurement of the left-right forward-backward asymmetry [26]. Fig. 7 illustrates the dependence of the polar angular distribution on the polarization of the incoming electron beam. This measurement yields:

$$A_s = 0.85 \pm 0.06 \pm 0.07\,, \qquad (11)$$

in agreement with the SM prediction.

The forward-backward pole asymmetry of s-quarks is measured by DELPHI [27] to be:

$$A_{FB}^{0,s} = 0.1008 \pm 0.0113 \pm 0.0040\,. \qquad (12)$$

Cross sections and asymmetries of the other four quark flavours are fixed to their SM expectations. Measurements performed at three different cms energies are compared in Fig. 8 to the SM.

2.4. Measurements of the effective weak mixing angle $\sin^2\overline{\vartheta}_W$

The measured asymmetries at the Z discussed above can be compared in terms of the effective weak mixing angle $\sin^2\overline{\vartheta}_W$ (Fig. 9). Averaging all measurements yields:

$$\sin^2\overline{\vartheta}_W = 0.23151 \pm 0.00017\,. \qquad (13)$$

The relatively poor χ^2 value of $11.9/6$ is caused by the different tendencies of leptonic and hadronic, mainly $A_{FB}^{0,b}$ and $A_{FB}^{0,c}$, measurements, a consequence of the observation already made in section 2.3.

The world average of $\sin^2\overline{\vartheta}_W$ points to a low value of the Higgs mass as can be seen at the bottom of Fig. 9

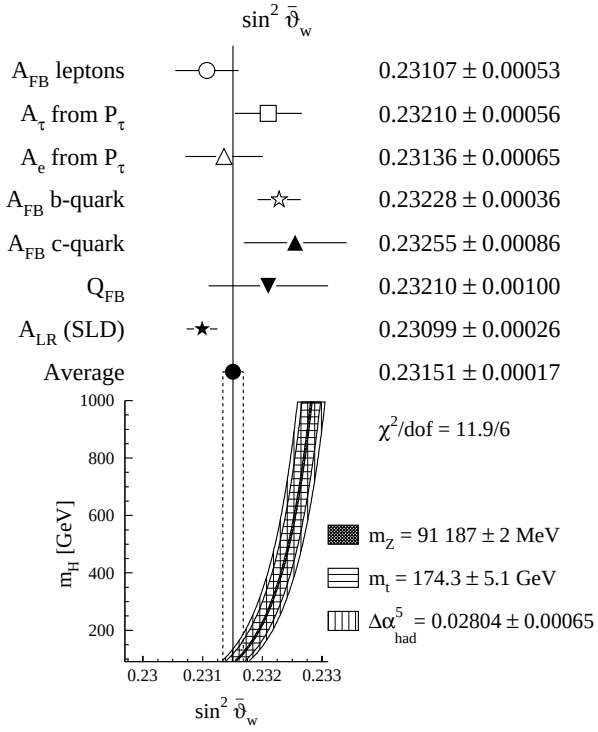

Figure 9. Measurements of the effective weak mixing angle $\sin^2\overline{\vartheta}_{\mathrm{W}}$ in various reactions at LEP and SLD. At the bottom the SM prediction is shown as a function of the Higgs boson mass. Uncertainties due to the knowledge of m_{t} and the contribution of the five light quarks to the running of α are shown as overlaid bands.

where the SM expectation is shown as function of m_{H}. Apart from the unknown Higgs mass, the knowledge of the top quark mass and, to an even larger extent, the contribution of the five light quarks to the running of the QED coupling constant, $\Delta\alpha^{(5)}_{\mathrm{had}}$, contribute to the uncertainty of the calculation of $\sin^2\overline{\vartheta}_{\mathrm{W}}$. This point will be addressed in section 6.

3. Fermion-pair production above the Z resonance

3.1. Measurements of total cross sections and forward-backward asymmetries at LEP

In the autumn of 1995 the LEP machine began to raise in steps the cms energy beyond the Z resonance. This has been possible after installation of additional super-conducting radio frequency cavities required to compensate the higher energy loss due to synchrotron radiation at higher beam energies. Tab. 5 summarises the approximate cms energies and luminosities collected by each experiment. Some results based on about 50 pb^{-1} at cms energies of 192 GeV and 196 GeV are included from the ongoing run in 1999.

Year	$\sqrt{s}$	$\int \mathcal{L}\,\mathrm{d}t$
1995	$130-140$ GeV	$5\ \mathrm{pb}^{-1}$
1996	$161/172$ GeV	$21\ \mathrm{pb}^{-1}$
1997	183 GeV	$55\ \mathrm{pb}^{-1}$
	$130/136$ GeV	$7\ \mathrm{pb}^{-1}$
1998	189 GeV	$180\ \mathrm{pb}^{-1}$
1999	192 GeV	$27\ \mathrm{pb}^{-1}$
	196 GeV	$20\ \mathrm{pb}^{-1}$

Table 5. Summary of the LEP operation above the Z resonance. Listed are the approximate cms energies and typical integrated luminosities collected by each experiment. For 1999 the integrated luminosities collected at the time of the conference are listed and for which some preliminary results were available [28].

The LEP experiments study fermion pair production at cms energies far above the Z resonance in the same channels as at the Z pole (Eq.1) [29, 30]. However, at high energies the total cross sections are about two orders of magnitude smaller.

At cms energies above the Z pole initial state radiation plays an important role. Radiation of one or more photons by the incoming electrons removes energy from the annihilation process and the fermion production takes place at a lower effective cms energy, $\sqrt{s'}$, where the cross section is different. In particular, if the remaining energy in the $\mathrm{e^+e^-}$ system is close to the mass of the Z the annihilation cross section is very high. Consequently this provides a major contribution to the total cross section $\mathrm{e^+e^-} \to \mathrm{f\bar{f}}$ and it is called radiative 'return-to-the-Z'.

The importance of the return-to-the Z is illustrated in Fig. 10 which shows the distribution of the effective cms energy for LEP energies above the Z pole. Besides the peak at the nominal cms energy, with a smooth tail towards lower energies from the radiation of soft photons, one observes that a large fraction of the events is indeed produced at $\sqrt{s'} \approx m_{\mathrm{Z}}$.

Because of the different nature of events produced close to the nominal cms energy and those stemming from decays of real Z bosons, the LEP experiments measure two sets of cross sections and forward-backward asymmetries: for the total sample and the high energy events separated by a cut in the reconstructed $\sqrt{s'}$ value, in general $\sqrt{s'/s} > 0.85$.

The results of the total cross section measurements from the Z up to 196 GeV from DELPHI are shown in Fig. 11 for both the total event sample and the events at high $\sqrt{s'}$. The measurements are compared to the SM expectations as calculated with the program

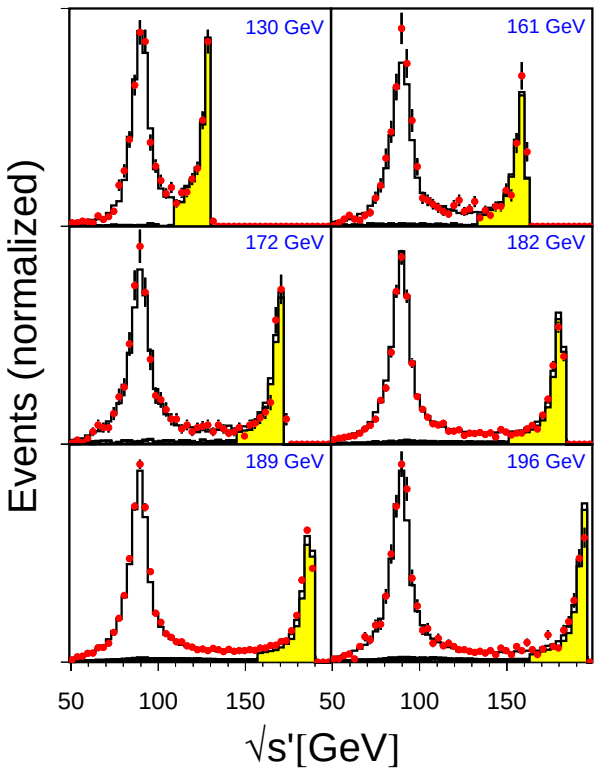

Figure 10. Distributions of the reconstructed effective cms energy in $e^+e^- \to$ hadrons at various cms energies of LEP. The dots are L3 data and the histograms represent Monte Carlo calculations. The shaded areas correspond to $\sqrt{s'/s} > 0.85$.

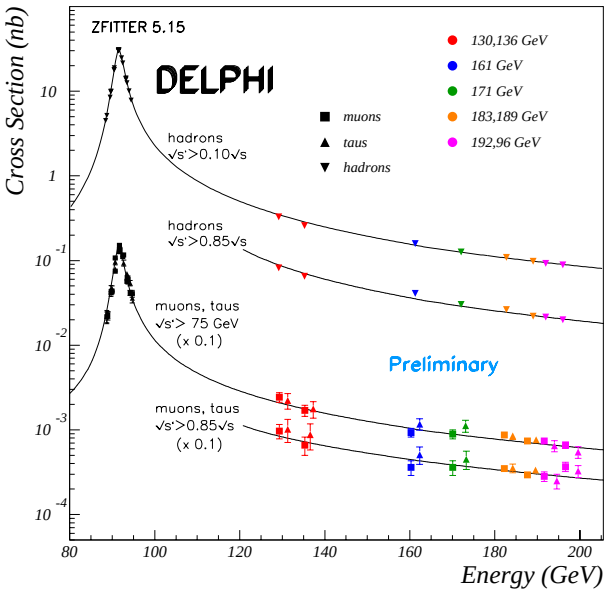

Figure 11. The cross sections for quark, muon and tau pair production as function of the cms energy measured by DELPHI from the Z resonance up to 196 GeV. Above the Z resonance results for the inclusive and the high effective cms energy samples are shown and compared to the SM.

ZFITTER. Similarly, Fig. 12 shows the forward-backward asymmetry in muon- and tau-pair production. Good agreement is observed between the measurements and the SM prediction.

Because of the low cross sections the measurements are statistically limited and precision is gained by combining the LEP experiments [31, 32]. The combinations are performed on the high energy event samples and the results are shown in Figs. 13 and 14. A precision as high as one percent is reached on the hadronic cross section at $\sqrt{s} = 189$ GeV. All measurements are in good agreement with the SM proving the electroweak unification above the Z resonance.

These measurements are used to put constraints on new physics. A general framework for the description of new phenomena are four-fermion contact interactions [33]. Lower limits on the energy scale of such contact interactions, to be considered as the mass scale of exchanged virtual particles, are set by the LEP experiments in the order of 10 TeV. Constraints on specific models beyond the SM derived from fermion-pair production are presented in references [34, 35].

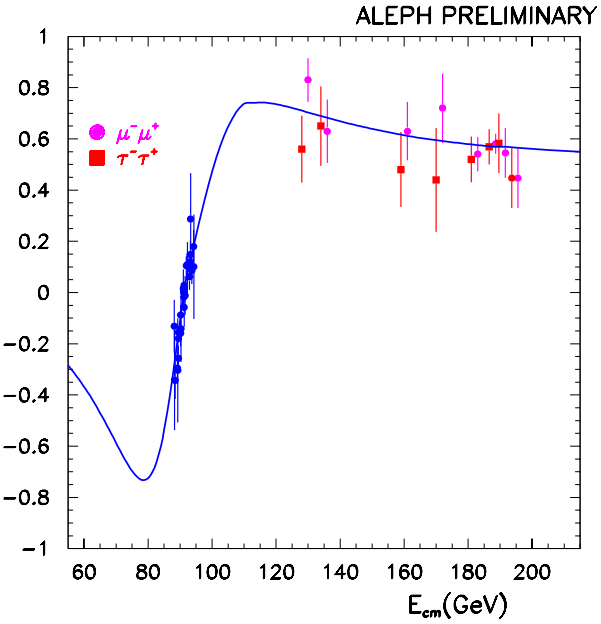

Figure 12. Measurements of forward-backward asymmetries in $e^+e^- \to \mu^+\mu^-$ and $e^+e^- \to \tau^+\tau^-$ by ALEPH for high effective cms energies, $\sqrt{s'}/\sqrt{s} > 0.9$.

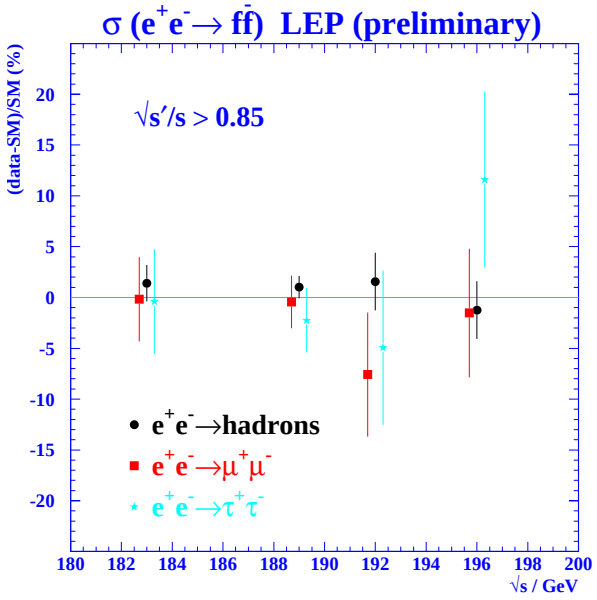

Figure 13. Combination of cross section measurements at LEP for 183 GeV $\leq \sqrt{s} \leq$ 196 GeV. Shown are the relative differences of the combined results to the SM expectations.

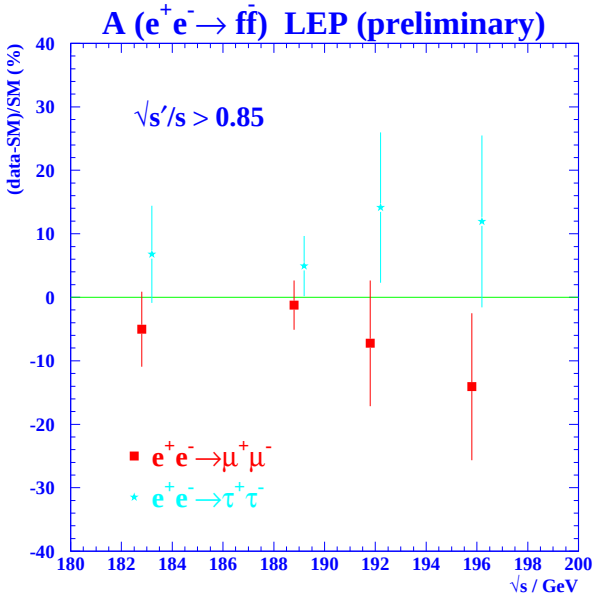

Figure 14. Same as Fig. 13 for the forward-backward asymmetry.

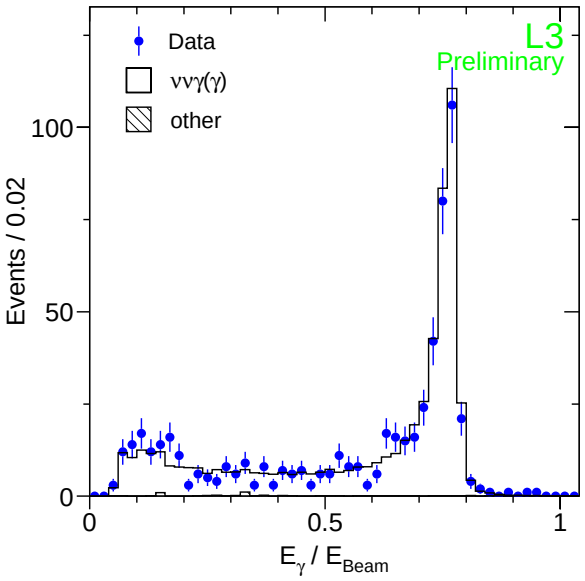

Figure 15. Energy spectrum of single photon events observed by L3 at $\sqrt{s} = 189$ GeV compared to the Monte Carlo expectation.

	$\sigma^{\rm meas}/\sigma^{\rm SM}$
ALEPH	0.984 ± 0.053
DELPHI	0.959 ± 0.069
L3	0.994 ± 0.045
OPAL	0.908 ± 0.054
LEP	0.965 ± 0.028

Table 6. Measurements of ratios of single photon cross sections to the SM expectations at $\sqrt{s} = 189$ GeV and the combined LEP result.

3.2. Single photon events and the number of neutrino families

An analysis which profits from the presence of the radiative return-to-the-Z is the study of the reaction $e^+e^- \to \nu\bar{\nu}\gamma$. This process gives rise to high energy single photons in the detector. At $\sqrt{s} = 189$ GeV about 500 such events are observed by each experiment and as an example the photon energy spectrum observed by L3 is shown in Fig. 15. Because of different cuts on the minimum photon energy and angular acceptances the LEP experiments cannot be compared directly. Tab. 6 therefore shows the ratio of measured and expected cross sections at $\sqrt{s} = 189$ GeV [36, 37]. Good agreement with the SM is observed. The cross section, for photons within the polar angular range $\cos\theta_\gamma \leq 0.97$ and with $E_\gamma > 5$ GeV, as a function of the cms energy is shown in Fig. 16.

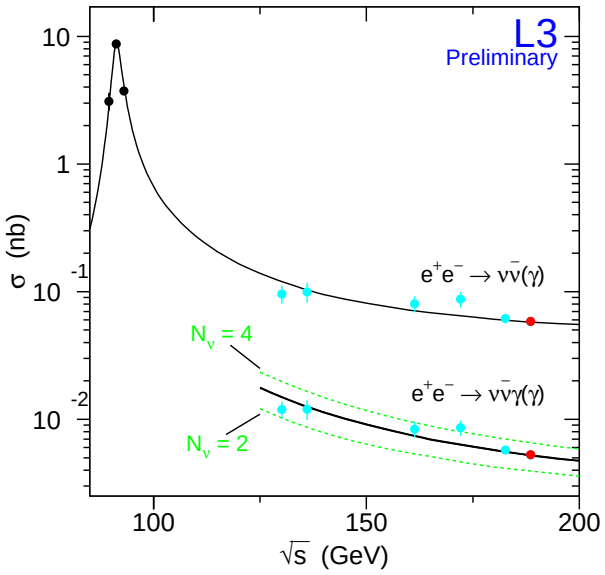

Figure 16. Cross section measurement $e^+e^- \to \nu\bar{\nu}\gamma$ above the Z resonance compared to the expectations for 2, 3 and 4 neutrino species. The upper curve shows the extrapolated, full cross sections $e^+e^- \to \nu\bar{\nu}$ from the Z resonance to $\sqrt{s} = 189$ GeV.

	N_ν
L3	3.05 ± 0.12
DELPHI	2.83 ± 0.19
LEP II	2.99 ± 0.10
LEP I	3.00 ± 0.08

Table 7. Determination of the number of neutrino generations from the analysis of single photon events above the Z resonance. The combined value (LEP II) is compared to the average result from similar analyses at the Z pole (LEP I) [38, 39].

The number of neutrino generations can be derived from this measurement. Tab. 7 shows results obtained above the Z resonance. The precision is comparable to the result derived from this reaction at the Z resonance, even though it is less precise than the measurement deduced from the Z lineshape (Eq. 5).

3.3. Production of b- and c-quarks

Employing techniques similar to those used at the Z resonance, b- and c-quarks are identified in hadronic events allowing the measurements of cross sections and forward-backward asymmetries [40]. Cross section measurements are expressed in terms of R_q which above the Z resonance is defined as ratio of individual quark

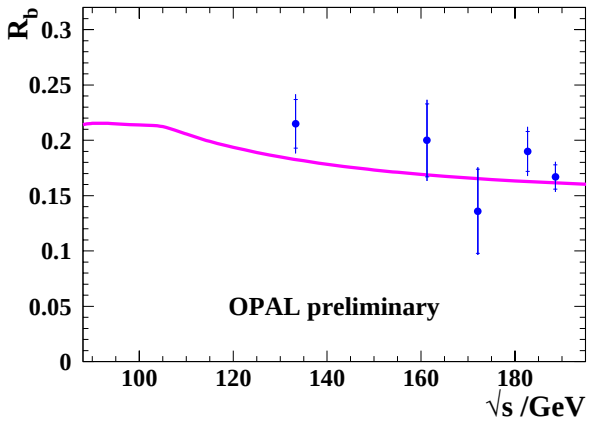

Figure 17. Measurements of R_b above the Z resonance by OPAL compared to the SM.

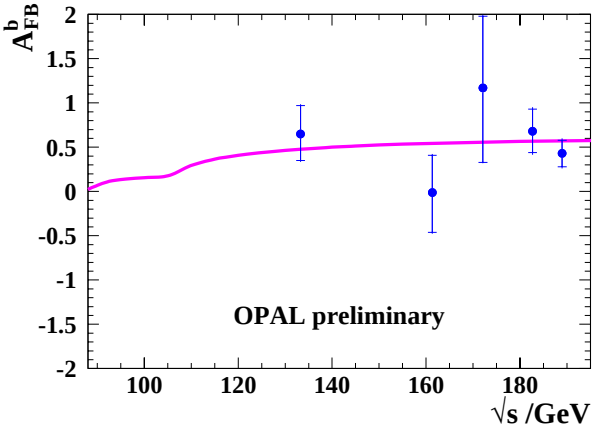

Figure 18. Same as Fig. 17 for the b-quark forward-backward asymmetry.

	R_b	A_FB^b
ALEPH	0.151 ± 0.011	0.34 ± 0.19
DELPHI	0.167 ± 0.012	—
L3	0.163 ± 0.016	0.66 ± 0.24
OPAL	0.167 ± 0.014	0.43 ± 0.17
LEP	0.161 ± 0.007	0.44 ± 0.12
SM	0.168	0.58

Table 8. Measurements of R_b and A_FB^b at $\sqrt{s} = 189$ GeV. The combined LEP measurements are compared to the SM expectations.

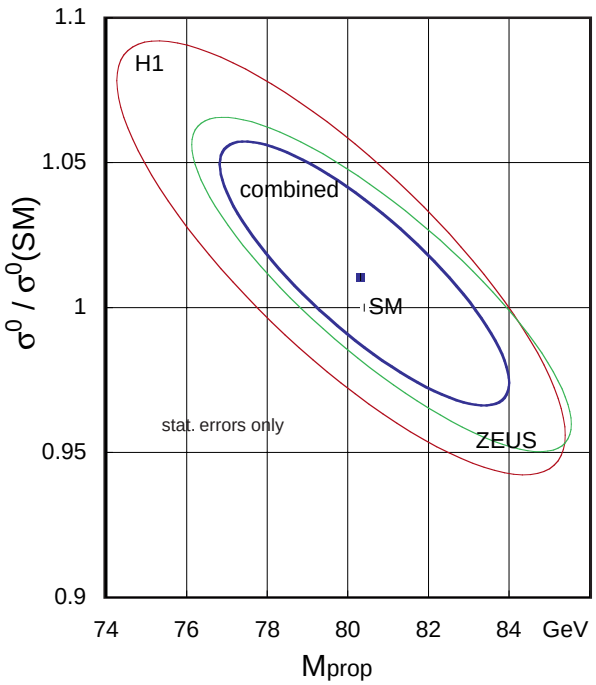

Figure 19. Contours in the plane of measured charged current cross section, normalized to the SM, and propagator mass. Shown are the results obtained by the two experiments and the combined contour.

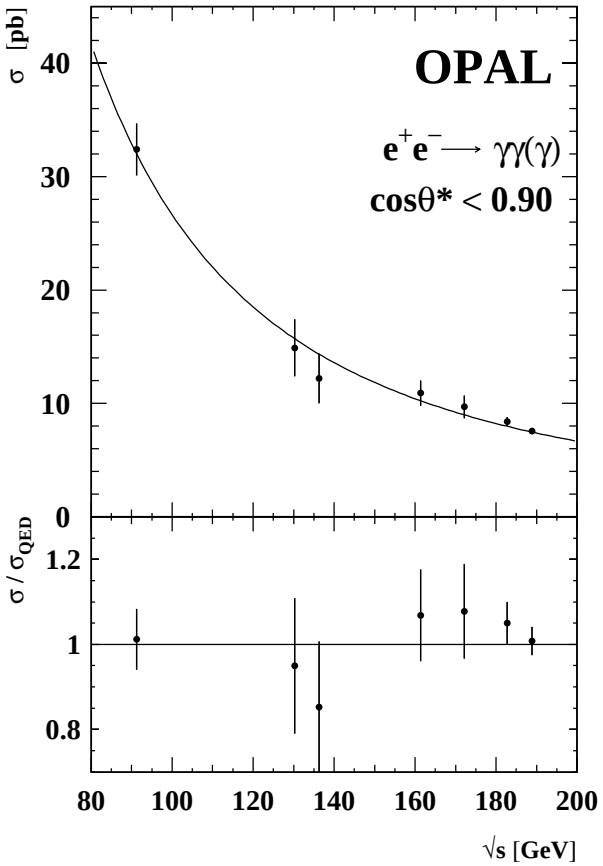

Figure 20. Measurements of the cross section $\mathrm{e^+e^-} \to \gamma\gamma$ by OPAL between the Z resonance and $\sqrt{s} = 189$ GeV. The solid curves is the SM expectation and the bottom shows the ratio between measurement and SM.

cross sections to the sum of the five flavours produced at LEP. Only events with high effective cms energy are considered in these analyses.

The measurements of R_b and A_FB^b by OPAL as function of the cms energy are shown in Figs. 17 and 18. The most precise measurements are performed at $\sqrt{s} = 189$ GeV (Tab. 8) and the combined LEP values agree with the expectations.

3.4. Electroweak tests at HERA

At LEP the time-like exchange of the photon and the Z is tested up to momentum transfers of $Q^2 \approx 40\,000\,\mathrm{GeV}^2$. In a complementary way at the HERA ep-collider the space-like exchange of W bosons is probed in a wide range of Q^2, reaching values comparable to LEP [41]. From the measured Q^2 dependence of charged current events the mass of the exchanged particle M_prop can be extracted:

$$\frac{\mathrm{d}\sigma}{\mathrm{d}Q^2} \propto \left(\frac{M_\mathrm{prop}^2}{M_\mathrm{prop}^2 + Q^2} \right)^2 . \qquad (14)$$

The results of the two experiments H1 and ZEUS together with the combination are shown in Fig. 19 as contours in the plane of measured cross section normalized to the SM expectation and the propagator mass. Mass values of

$$\begin{aligned} \mathrm{M_{prop}} &= 80.9 \pm 3.3 \pm 1.7 \pm 3.7\ \mathrm{GeV} \quad (\mathrm{H1})\,, \\ \mathrm{M_{prop}} &= 81.4\,^{+2.7}_{-2.6} \pm 2.0\,^{+3.3}_{-3.0}\ \mathrm{GeV} \quad (\mathrm{ZEUS}) \end{aligned} \qquad (15)$$

are derived from these measurements which are consistent with the exchange of W bosons. The quoted errors are statistical, experimental systematic and from uncertainties of the parton density functions.

4. Production of neutral boson pairs at LEP

4.1. Test of QED in $\mathrm{e^+e^-} \to \gamma\gamma$

Tests of Quantum Electrodynamics (QED) at the highest energies are possible at LEP by studying photon-pair production $\mathrm{e^+e^-} \to \gamma\gamma$. Measurements of total and differential cross sections are performed [42, 43] and good agreement with the QED prediction is found up

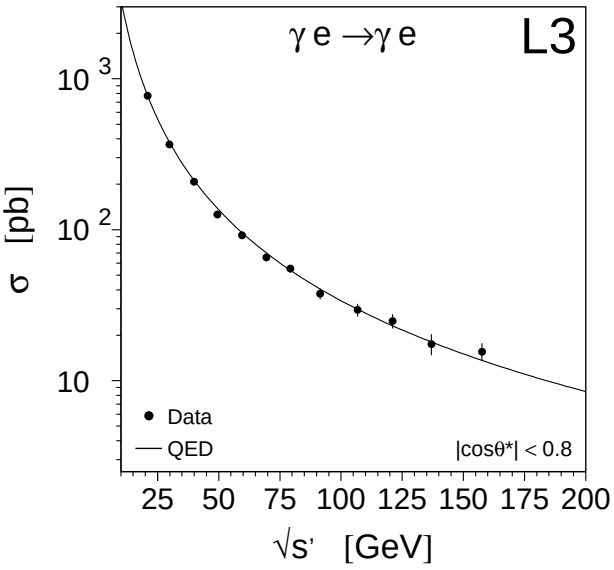

Figure 21. Measured Compton scattering cross section $e\gamma \to e\gamma$ as function of the energy in the electron-photon system, $\sqrt{s'}$. Data taken at cms energies from the Z resonance up to $\sqrt{s} = 189$ GeV are used.

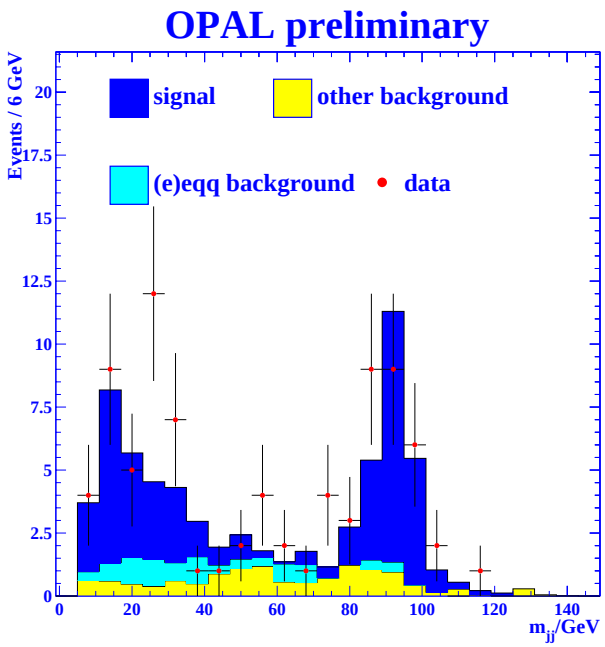

Figure 22. Distribution of the jet-pair mass in $e^{\pm}\gamma \to e^{\pm} Z/\gamma^*$ candidates observed by OPAL.

to the highest cms energy attained [28]. Fig. 20 shows as an example the total cross section measured by OPAL from the Z resonance up to $\sqrt{s} = 189$ GeV. From these analyses the experiments set lower limits on QED cut-off parameters $\lambda_{\pm}$ and on the mass of an excited electron of the order of 300 GeV [34].

4.2. Electron-photon scattering

Another pure QED process studied at LEP is the Compton scattering of quasi-real photons with electrons, $e^{\pm}\gamma \to e^{\pm}\gamma$ [44]. The low virtuality of the initial state photon is ensured by imposing a cut on the reconstructed transverse momentum of the electron it was radiated off. Approximately 6000 events are observed in the data collected between the Z resonance and 189 GeV by the L3 experiment. The cross section of this process as a function of the energy in the system of the scattering electron and photon is measured as shown in Fig. 21. Good agreement up to an energy of 160 GeV in the electron-photon system is observed which constraints the mass and coupling of an excited electron [34].

A similar process, electroweak Compton scattering, where the scattering of the photon results in the production of a Z boson or a highly virtual photon, $e^{\pm}\gamma \to e^{\pm} Z/\gamma^*$, is studied by the OPAL collaboration [45]. The decays of the Z or the γ^* into hadrons are investigated and the invariant mass distribution of the jet pairs as shown in Fig. 22 is observed. The shape and absolute rate measured in the data is in agreement with the expectation allowing a clear distinction between virtual photons, $m_{\mathrm{jj}} < 60$ GeV, and the single Z production.

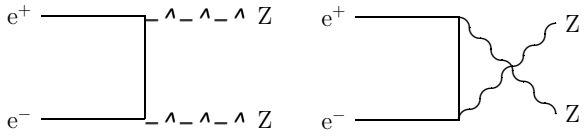

Figure 23. Feynman diagrams contributing to $e^+e^- \to ZZ$ at lowest order.

4.3. Production of Z-boson pairs

With the cms energy increased to 183 GeV in 1997, LEP has attained the threshold for Z-pair production, $e^+e^- \to ZZ$. In the SM this process is mediated by t- and u-channel exchange of an electron with two Feynman diagrams contributing in lowest order (Fig. 23). Candidate events are selected as four-fermion final states requiring that the reconstructed invariant masses of jet and lepton pairs are consistent with the production of real Z bosons. The sum of the two invariant masses in candidate events of DELPHI collected at $\sqrt{s} = 189$ GeV is shown in Fig. 24. The presence of a $e^+e^- \to ZZ$ signal is clearly visible in the data.

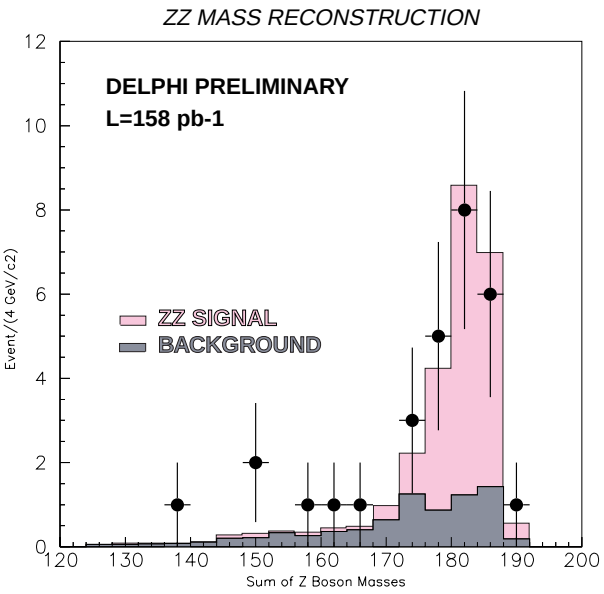

Figure 24. Distribution of the sum of the two reconstructed invariant masses in $e^+e^- \to ZZ$ candidates of DELPHI.

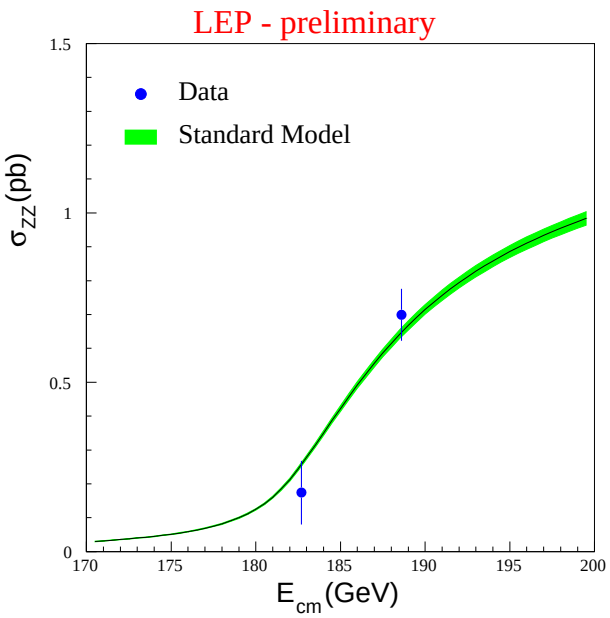

Figure 25. Combined LEP cross section measurements of $e^+e^- \to ZZ$ at two cms energies compared to the SM expectation.

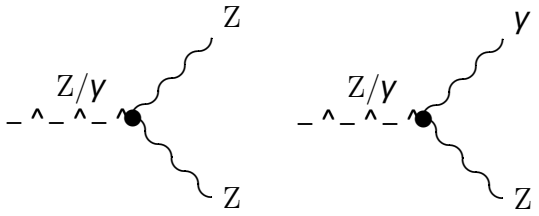

Figure 26. Anomalous couplings among neutral gauge bosons to be studies in Z-pair (left) and in Z-photon production (right).

Evidence for this process was established before using the data at 183 GeV [46, 47]. Now, due to the increased cross section and higher luminosity accumulated at $\sqrt{s} = 189$ GeV, several dozens of candidates are collected by each experiment allowing a respectable cross section measurement [47–49]. The combined LEP measurements are shown in Fig. 25 confirming the SM.

4.4. Z-photon final states and limits on anomalous couplings

The good agreement of the measured Z-pair cross section with the expectation can be expressed in limits on ZZZ and ZZγ couplings which do not exist in the SM at tree level (Fig. 26). In a general ansatz, couplings at these vertices are parametrized by four complex parameters [50]: f_i^V, $V = \mathrm{Z}, \gamma$, $i = 4, 5$.

More information on anomalous Z-photon couplings is extracted from analyses of $e^+e^- \to f\bar{f}\gamma$ (Fig. 26) [51] and $p\bar{p} \to Z\gamma$ [52] events. In these cases eight parameters† are needed to describe the ZZγ and Z$\gamma\gamma$ vertices in a general way [50]: h_i^V; $V = \gamma, \mathrm{Z}$, $i = 1, \ldots, 4$.

At LEP rate and spectra of $e^+e^- \to \mathrm{hadrons} + \gamma$ and single photon (Fig. 15) events are analyzed. They are found to agree with the expectations as well as the study of Zγ events in $p\bar{p}$ collisions done by DØ. Figs. 27 and 28 compare limits on the CP conserving coupling parameters h_3^V and h_4^V obtained by L3 and DØ. Due to the different energy dependence of the effects caused by these parameters the results obtained at LEP and by DØ are complementary.

A compilation of limits on Zγ coupling parameters is shown in Tab. 9.

† There is no constraint of two identical particles in the final state as in $e^+e^- \to ZZ$. Also, the f_i^γ and h_i^Z parametrizing the ZZγ vertices are independent because of different particles in the propagators.

5. The properties of the W boson

5.1. Production of W boson pairs at LEP

The production of W bosons pairs, $e^+e^- \to W^+W^-$, is studied by the LEP experiments since the threshold energy was reached in 1996. In the first three years about 3500 W-pair events have been collected by each of the four experiments in the cms energy range $161\ \mathrm{GeV} \leq \sqrt{s} \leq 189\ \mathrm{GeV}$.

$e^+e^- \to ZZ$		
DELPHI:	$-2.7 < f_4^Z < +2.7$	$-1.6 < f_4^\gamma < +1.6$
	$-7.1 < f_5^Z < +5.7$	$-3.9 < f_5^\gamma < +3.9$
L3:	$-1.9 < f_4^Z < +1.9$	$-1.1 < f_4^\gamma < +1.1$
	$-4.9 < f_5^Z < +4.7$	$-3.0 < f_5^\gamma < +2.9$
OPAL:	$-2.0 < \Re\{f_4^Z\} < +2.0$	$-1.2 < \Re\{f_4^\gamma\} < +1.2$
	$-5.1 < \Re\{f_5^Z\} < +5.1$	$-3.2 < \Re\{f_5^\gamma\} < +3.0$
	$-2.0 < \Im\{f_4^Z\} < +1.9$	$-1.2 < \Im\{f_4^\gamma\} < +1.2$
	$-5.2 < \Im\{f_5^Z\} < +5.4$	$-3.2 < \Im\{f_5^\gamma\} < +3.0$

$e^+e^- \to q\bar{q}\gamma$, $\nu\bar{\nu}\gamma$ and $p\bar{p} \to Z\gamma + X$		
DELPHI*:	$\lvert h_{30}^Z\rvert < 0.38$	$\lvert h_{30}^\gamma\rvert < 0.23$
L3:	$-0.09 < h_1^Z < 0.20$	$-0.09 < h_1^\gamma < 0.08$
	$-0.12 < h_2^Z < 0.06$	$-0.05 < h_2^\gamma < 0.07$
	$-0.16 < h_3^Z < 0.15$	$-0.09 < h_3^\gamma < 0.07$
	$-0.09 < h_4^Z < 0.10$	$-0.05 < h_4^\gamma < 0.06$
DØ**:	$\lvert h_{30}^Z\rvert < 0.36$	$\lvert h_{30}^\gamma\rvert < 0.37$
	$\lvert h_{40}^Z\rvert < 0.05$	$\lvert h_{40}^\gamma\rvert < 0.05$

* $\Lambda = 1000$ GeV ** $\Lambda = 750$ GeV

Table 9. Summary of limits (95% CL) on anomalous Z-photon couplings. If not stated otherwise limits are derived for the real part of the coupling. Limits on h_i^V are posed assuming no form-factor dependence or a dependence on the energy scale of new physics Λ as $h_i^V = h_{i0}^V/(1 + s/\Lambda^2)^n$ with $n = 3$ for $i = 1, 3$ and $n = 4$ for $i = 2, 4$ [53].

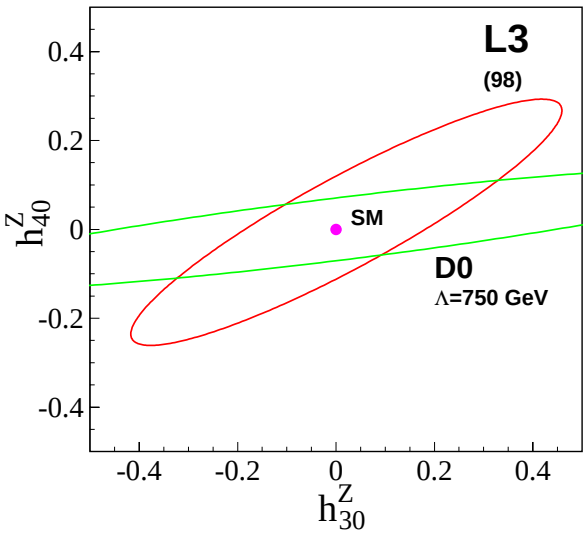

Figure 27. Limits at 95% CL on anomalous ZZγ couplings h_{40}^Z and h_{30}^Z obtained by L3 and DØ.

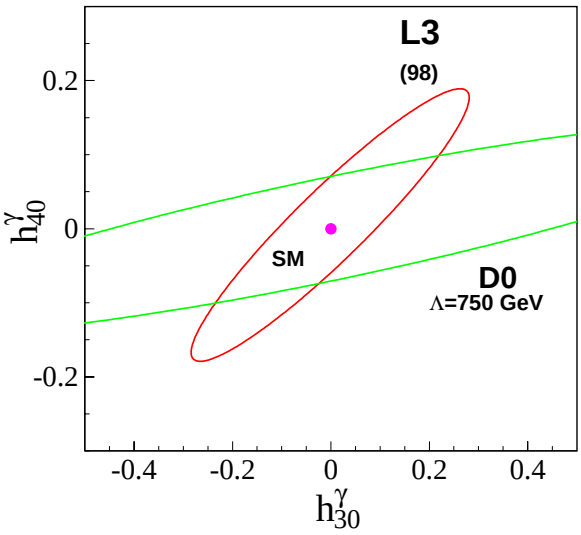

Figure 28. Same as Fig. 27 for anomalous Z$\gamma\gamma$ couplings h_{40}^γ and h_{30}^γ.

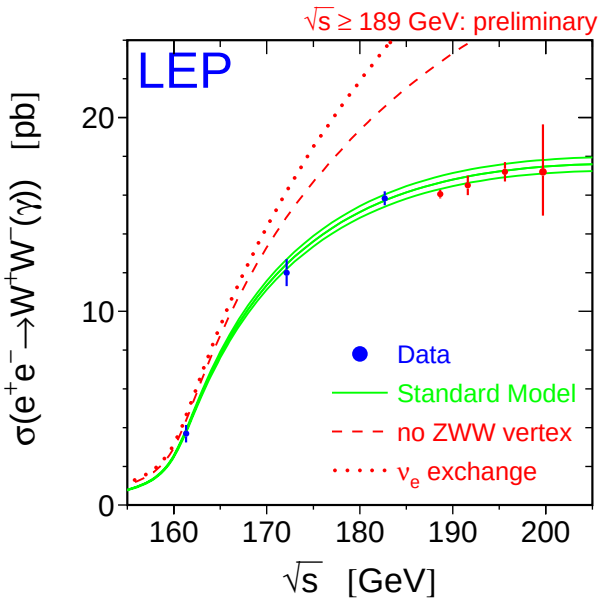

Figure 29. The combined LEP cross section measurements $e^+e^- \to W^+W^-$ at cms energies between 161 GeV and 200 GeV. The band shows the SM prediction, calculated with KORALW [56], and its uncertainty. The dashed lines represent hypotheses without ZWW coupling and for neutrino exchange only.

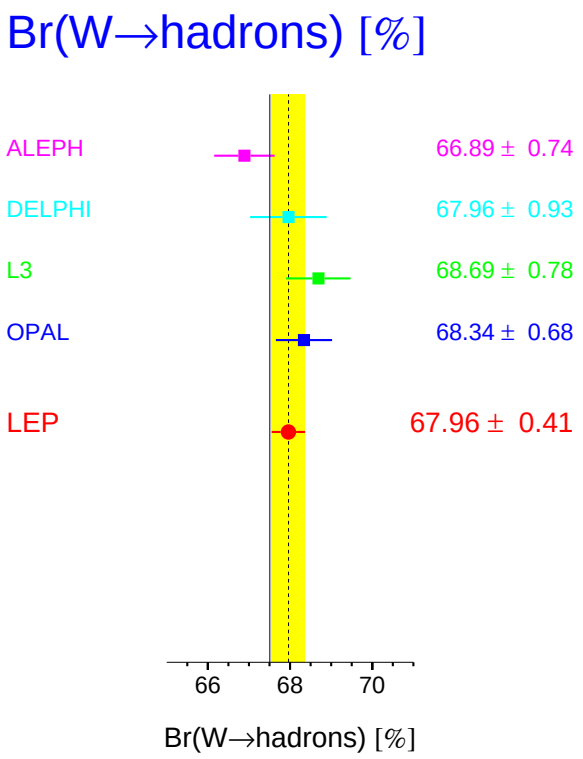

Figure 30. Measurements of the branching ratio $W \to$ hadrons at LEP. The solid vertical line shows the SM expectation.

Three different topologies are distinguished in the analysis of W-pair events: purely leptonic $e^+e^- \to \ell\nu\ell\nu$ ($\ell = e, \mu, \tau$), which contribute about 11%, semi-leptonic $e^+e^- \to q\bar{q}\ell\nu$ (44%) and fully hadronic final states $e^+e^- \to q\bar{q}q\bar{q}$ (45%). While the leptonic W decays can be identified with high efficiency and low background contributions from other processes, the separation of $W^+W^- \to q\bar{q}q\bar{q}$ events from QCD four-jet production is more difficult [54, 55].

The average cross sections measured by the LEP experiments as a function of the cms energy is shown in Fig. 29 [57]. The graph includes very recent measurements from the 1999 run based on analyzed luminosities as given in Tab. 5 [28]. The measurements follow the SM prediction which at the moment has an uncertainty of 2% as indicated in the figure. Improved calculations are being performed which should reduce this uncertainty to about 0.5% in near future [58].

The measurements performed at LEP rule out hypotheses with no ZWW vertex or only t-channel exchange of electron neutrinos in W-pair production and prove the existence of triple gauge boson couplings. The large gauge cancellation predicted by the SM to remove the divergences of the individual diagrams contributing to $e^+e^- \to W^+W^-$ are now confirmed by experiments.

5.2. W branching ratios and lepton universality in charged current interactions

From the observed rates of W decays into hadrons and the three lepton species the W branching ratios are determined. Fig. 30 lists the results for the hadronic branching ratio obtained by the LEP experiments, using data up to $\sqrt{s} = 189$ GeV, together with the average and the SM expectation.

The hadronic branching ratio depends on the six elements of the Cabbibo-Kobayashi-Maskawa (CKM) matrix not involving the top quark [59]. By fixing five of them to the world averages [38] the least precise of the two diagonal elements is derived to be $|V_{cs}| = 0.997 \pm 0.020$.

By tagging charm quarks in W decays the decay width $\Gamma(W \to cX)$ is measured directly and $|V_{cs}|$ can be derived. Results on $R_c = \Gamma(W \to cX)/\Gamma(W \to \text{hadrons})$ and $|V_{cs}|$ are listed in Tab. 10.

Measurements of the W branching ratios into the three lepton families are summarized in Fig. 31. The individual results of the four experiments are given together with the average values for the three lepton types. These three branching fractions are the same

	R_c	$\lvert V_{cs}\rvert$
ALEPH*	$0.51 \pm 0.05 \pm 0.03$	$1.00 \pm 0.11 \pm 0.07$
OPAL	$0.47 \pm 0.04 \pm 0.06$	$0.91 \pm 0.07 \pm 0.11$

* 183 GeV data only

Table 10. Measurements at LEP of the ratio of the W decay width into c-quarks and the total hadronic width [60, 61]. The CKM matrix element $|V_{cs}|$ derived from these measurements are listed in the right-most column.

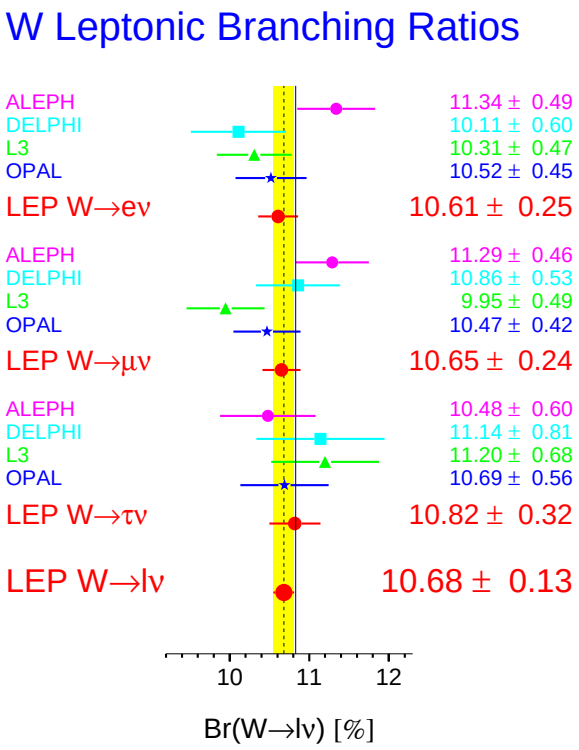

Figure 31. Measurements of the W branching ratios into the three lepton species performed by the LEP experiments together with the combined leptonic branching ratio $W \to \ell\nu$. The solid vertical line shows the SM expectation.

within their errors yielding a value of $10.68 \pm 0.13\%$ for the leptonic branching ratio which agrees within one standard deviation with the SM prediction. The test of lepton universality in charged current interactions at the scale of the W mass can be quantified by forming ratios of the charged current coupling constants as derived from the measured branching fractions at LEP:

$$\begin{aligned} g_\mu/g_e &= 1.001 \pm 0.016\,, \\ g_\tau/g_e &= 1.010 \pm 0.022\,, \\ g_\tau/g_\mu &= 1.008 \pm 0.021\,. \end{aligned} \qquad (16)$$

The branching ratio $W \to e\nu$ is measured by CDF and DØ to be $10.37 \pm 0.22\%$ and $10.80 \pm 0.30\%$ [62] and from identified $W \to \tau\nu$ decays DØ measures the ratio of coupling constants to be $g_\tau/g_\mu = 0.98 \pm 0.03$.

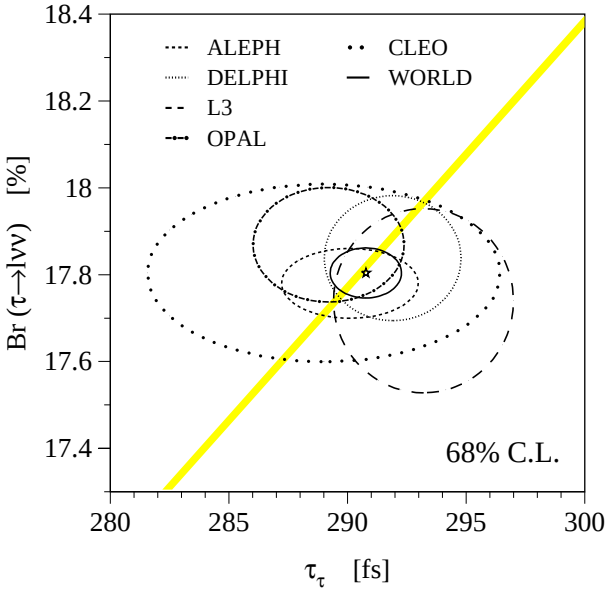

Figure 32. Measurements of the leptonic branching ratio and the lifetime of the tau at LEP and by the CLEO experiment. The combined contour is also shown with the star indicating the central values. The band represents the SM relation of the parameters with its uncertainty.

More stringent tests of lepton universality in charged current interactions are performed at the scale of the tau mass using the measurements of the leptonic branching ratios and the tau lifetime. Including new results [63–65] the world averages are obtained to be [66]†:

$$\begin{aligned} BR(\tau \to e\,\nu_e\,\nu_\tau) &= (17.791 \pm 0.054)\%\,, \\ BR(\tau \to \mu\,\nu_\mu\,\nu_\tau) &= (17.333 \pm 0.054)\%\,, \\ BR(\tau \to \ell\,\nu_\ell\,\nu_\tau) &= (17.805 \pm 0.039)\%\,, \\ \tau_\tau &= 290.77 \pm 0.99\ \text{fs}\,. \end{aligned} \qquad (17)$$

Measurements from the LEP collaborations and from CLEO of the tau leptonic branching ratio and lifetime are presented as contours in Fig. 32.

By comparing the tau branching ratios into electrons and muons the equality of their coupling constants to the W boson is tested [67]. Likewise, universality of tau and muon is verified by comparing the tau decay width into electrons, derived from the measured branching ratio and lifetime, to the muon decay width. Both results,

† The average leptonic branching ratio $BR(\tau \to \ell\,\nu_\ell\,\nu_\tau)$ corresponds to a massless lepton ℓ.

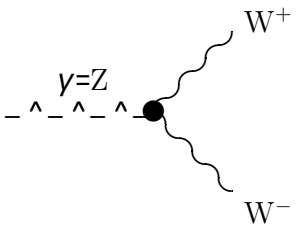

Figure 33. γWW and ZWW vertex.

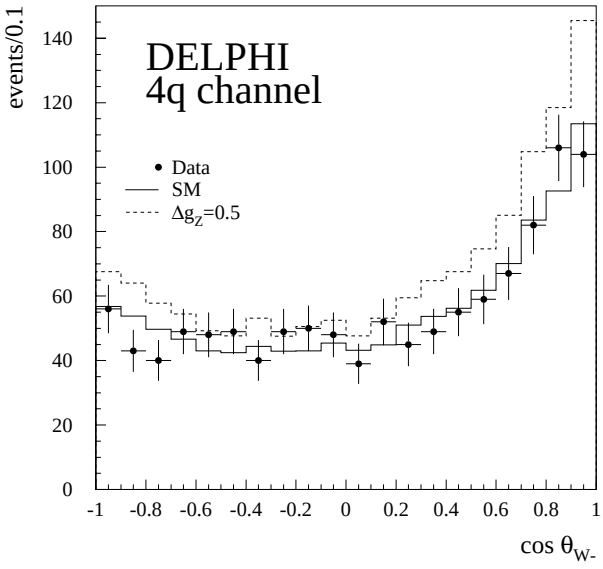

Figure 34. Polar angular distribution of W bosons in fully hadronic W-pair decays as observed by DELPHI. The data are compared to the SM expectation and to the hypothesis $g_1^Z = 1.5$.

expressed in ratios of coupling constants,

$$g_\mu/g_e = 1.0006 \pm 0.0023\,, \qquad g_\tau/g_\mu = 0.9997 \pm 0.0024\,, \tag{18}$$

confirm universality in charged current interactions at the scale of the tau mass at the permille level.

5.3. The couplings of the W boson

The non-abelian structure of the SM predicts the existence of couplings between the gauge bosons, in particular the triple gauge boson vertices γWW and ZWW. Their existence is unambiguously confirmed by the measurements of the cross section $e^+e^- \to W^+W^-$ at LEP (Fig. 29). More detailed studies of the triple gauge boson couplings are performed by exploiting the additional information contained in differential distributions of W boson production and decay angles.

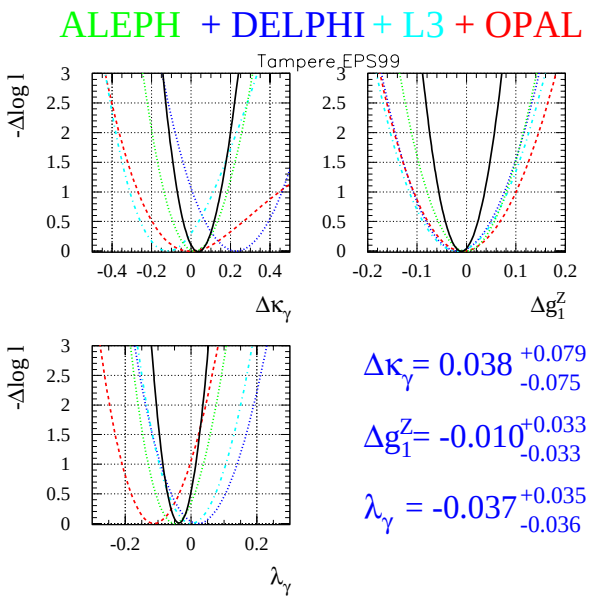

Figure 35. Results on triple gauge boson couplings obtained at LEP from studies of $e^+e^- \to W^+W^-$ up to $\sqrt{s} = 189$ GeV. Shown are likelihood curves obtained by the four experiments from fits to the total and differential cross sections together with the combined results (solid lines). The symbol Δ denotes the difference to the SM expectation as given in Eq. 19. In the bottom right corner the central values with the 68% CL errors are listed.

In the most general Lorentz invariant ansatz the γWW and ZWW vertices are parametrized by 2×7 complex couplings [50]. Because these are too many parameters to be measured simultaneously, real couplings as well as C, P and CP invariance are assumed. Imposing also $SU(2)$ symmetry three coupling parameters remain to be studied [68]: g_1^Z, κ_γ, λ_γ. These parameters do not affect the gauge boson propagators at tree level which would lead to effects observable at the Z resonance. The parameter g_1^Z describes the ZWW coupling and the other two are related to the static magnetic dipole and electric quadrupole moment of the W boson†. The SM values for these couplings are given as:

$$g_1^Z = 1, \quad \kappa_\gamma = 1, \quad \lambda_\gamma = 0\,. \tag{19}$$

Deviations from the SM would lead to an increased $e^+e^- \to WW$ cross section and to modified W production angles and polarization observable at LEP. An example is given in Fig. 34 which shows the polar angular distribution of the W boson.

Results on the three triple gauge boson couplings obtained at LEP from studies of $e^+e^- \to W^+W^-$ are

† The relations are $\mu_W = \frac{e}{2m_W}(2 + \Delta\kappa_\gamma + \lambda_\gamma)$ and $Q_W = -\frac{e}{m_W^2}(1 + \Delta\kappa_\gamma - \lambda_\gamma)$, respectively.

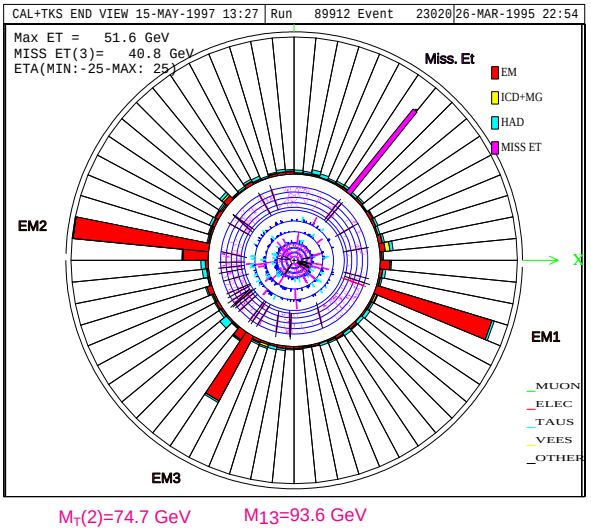

Figure 36. Candidate event $p\bar{p} \to WZ + X \to eee\nu + X$ observed in the DØ experiment. Shown are the energy deposits of the three electrons and, in the upper right part, the missing transverse momentum caused by the neutrino.

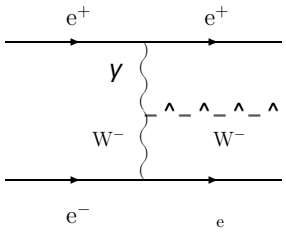

Figure 37. Feynman diagram of single W boson production.

shown in Fig. 35 [69, 70]. The likelihood curves are derived from fits to the measured total and differential cross sections leaving one coupling free and fixing the other two parameters to the SM expectation [71]. No deviations from the SM are observed and the triple gauge boson couplings are tested with a precision of a few percent.

At the Tevatron anomalous triple boson couplings would lead to an enhanced production of boson pairs $W\gamma$, WW or WZ. Fig. 36 shows a candidate event observed by DØ for WZ production in $p\bar{p}$ collisions. The observations are consistent with the SM yielding measurements of triple boson couplings with a precision comparable to a single LEP experiment by DØ [72]:

$$\Delta\kappa_\gamma = -0.08 \pm 0.34\,, \qquad \lambda_\gamma = 0.00\,^{+0.10}_{-0.09}\,. \quad (20)$$

At LEP additional information on triple gauge boson couplings is contained in the production of single W bosons. This process, sketched in Fig. 37, is

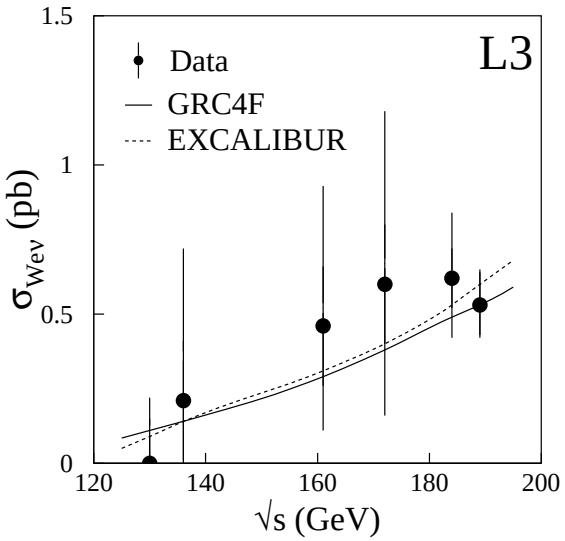

Figure 38. Single W boson cross section as a function of the cms energy measured by L3. The data are compared to the two Monte Carlo calculations GRC4F [73] and EXCALIBUR [74].

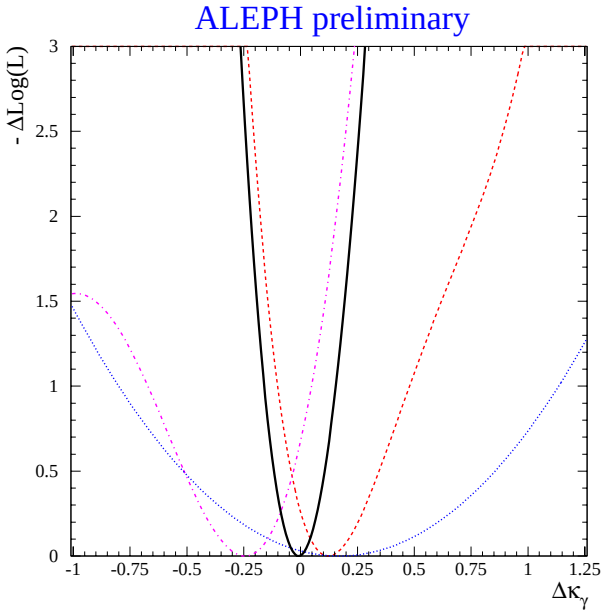

Figure 39. Measurement of the triple gauge boson coupling κ_γ by ALEPH. Shown are the likelihood curves obtained from W pairs (dashed), single W (dashed-dotted) and single photon (dotted) production as well as the sum (solid line).

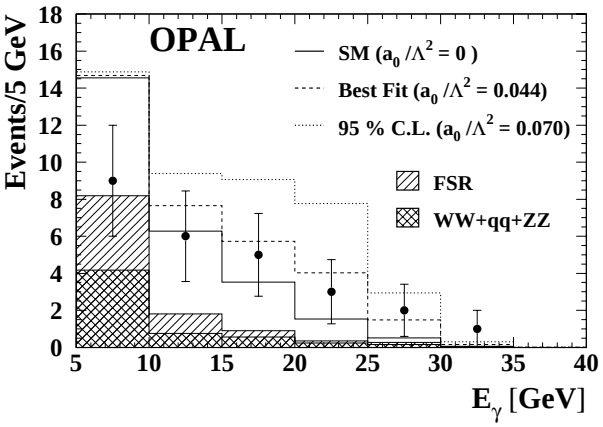

Figure 40. Photon energy spectrum in $e^+e^- \to W^+W^-\gamma$ events as measured by OPAL. The data are compared to the SM and to values of an anomalous quartic coupling a_0/Λ^2 not excluded by the measurement.

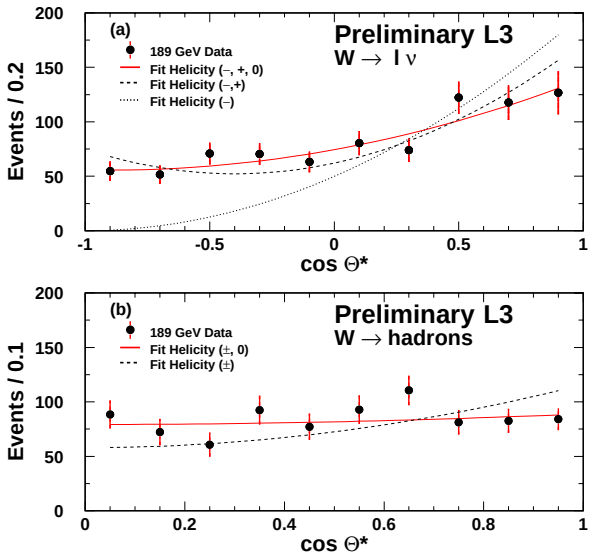

Figure 41. Polar angular distributions in the W boson rest frame as measured by L3. The plot shows the polar angle of the charged lepton in $W \to \ell\nu$ decays (top) and of the jets in hadronic decays (bottom). The lines represent the fit results allowing for transverse polarizations states $(+,-)$ only or including contributions from longitudinal (0) W bosons.

particularly sensitive to the parameter κ_γ. As this is a t-channel process, the final state electron typically escapes along the beam pipe producing spectacular two-jet or single-lepton events with missing energy. The small cross section of this reaction is measured by the LEP experiments [75, 76] and found to be in agreement with the SM. For example the cross section as function of the cms energy measured by L3 is shown in Fig. 38.

Also single photon final states contain information on the $WW\gamma$ vertex as can be seen from Fig. 37 interchanging the role of the W and the photon. The improved determination of κ_γ by ALEPH exploiting all three final states is shown in Fig. 39. The result is consistent with the SM: $\Delta\kappa_\gamma = -0.01\,^{+0.14}_{-0.11}$.

In the SM also quartic couplings among the gauge bosons exist. At LEP the vertices $WW\gamma\gamma$ and $WWZ\gamma$ can be studied in the reaction $e^+e^- \to W^+W^-\gamma$. However, their existence cannot be proven because at LEP energies the effect of the SM quartic couplings is much too small to be measurable. Hence only limits on anomalous contributions to the quartic gauge couplings are derived.

The first analysis of $e^+e^- \to W^+W^-\gamma$ is performed by OPAL and the observed photon spectrum is shown in Fig. 40 [77]. The photon rate and spectrum is in agreement with the SM calculations and the first direct limits on genuine quartic boson couplings [78] are obtained [79]:

$$\begin{aligned} -0.065\ \mathrm{GeV}^{-2} < \ & a_0/\Lambda^2 \ < +0.065\ \mathrm{GeV}^{-2}\,, \\ -0.13\ \mathrm{GeV}^{-2} < \ & a_c/\Lambda^2 \ < +0.17\ \mathrm{GeV}^{-2}\,, \\ -0.61\ \mathrm{GeV}^{-2} < \ & a_n/\Lambda^2 \ < +0.57\ \mathrm{GeV}^{-2}\,. \end{aligned} \quad (21)$$

To obtain these results also the reaction $e^+e^- \to \nu\bar{\nu}\gamma\gamma$ is exploited. More stringent indirect limits exist on a_0 and a_c which are derived from precision measurements at the Z resonance [80].

5.4. Longitudinally polarized W bosons

In addition to the two possible transverse polarization states of massless spin-one particles like the photon, the massive gauge bosons should exist also in the longitudinal helicity state. In the SM this polarization state is related to the mechanism of electroweak symmetry breaking in which three degrees of freedom of the scalar Higgs field generate the longitudinal helicity states of the $W^\pm$ and Z. Remarkably, only transverse W bosons are produced in weak processes involving light fermions. However, in pair production of W bosons at LEP a considerable contribution from longitudinal W bosons is expected [68] making this helicity state experimentally accessible.

The helicity states can be distinguished by the angular distributions of the W decay products. In the W rest frame the angle between the W and the charged lepton is proportional to $(1 \pm \cos\Theta^*)^2$ for transverse polarized W bosons while longitudinal W produce a symmetric distribution $\sin^2\Theta^*$. Fig. 41 shows this angular distribution for leptonic W decays and, symmetrized as no distinction between quarks and anti-quarks is attempted, for hadronic decays. The L3 measurements establish the admixture of longitudinal W bosons. Combining the $\sqrt{s} = 183$ GeV and $\sqrt{s} =$

189 GeV data the fraction of longitudinally polarized W bosons in $e^+e^- \to W^+W^-$ is measured to be [81] $0.261 \pm 0.051 \pm 0.03$ which compares well with the SM expectation of 0.26.

In decays of the heavy top quark 70% of the W bosons are expected to be produced in the longitudinal helicity state. From the observed transverse momentum spectrum in $t \to b\ell\nu$ decays CDF derives this fraction to be [82,83] $0.91 \pm 0.37 \pm 0.13$ establishing the existence of this helicity state also in top quark decays.

5.5. Measurement of the W mass at LEP

An important measurement for precision tests of the SM is the determination of the W mass. At LEP the large data sample collected in 1998 allows for a significant improvement of this measurement.

The mass of the W boson is determined from invariant mass distributions in $e^+e^- \to WW$ events [84]. To improve the mass resolution kinematic fits are employed imposing energy and momentum conservation. The four final states $q\bar{q}\,\ell\nu$, ($\ell = e, \mu, \tau$) and $q\bar{q}\,q\bar{q}$ are used. Examples of the mass distributions obtained from the 189 GeV data are shown in Fig. 42 [85]. The W mass is extracted by fitting re-weighted Monte Carlo to the observed distributions.

As the kinematic fit imposes energy conservation the absolute scale of the W mass is determined by the LEP beam energy. The method of resonant depolarization [86] cannot be applied above the W pair threshold. Magnetic extrapolations are required which limit the knowledge of the beam energy to a precision of $2{\cdot}10^{-4}$ at $\sqrt{s} = 189$ GeV [87–89] which causes an error of ± 17 MeV on m_W common to all LEP experiments.

A particular problem of the W mass measurement in $e^+e^- \to q\bar{q}\,q\bar{q}$ final states are interactions between the decay products of the two different W bosons: colour reconnection and Bose-Einstein correlations. Because the typical distance between the decay points of the two W bosons (0.1 fm) is much smaller than the hadronisation scale of the quarks (1 fm) gluons are exchanged between quarks from different W bosons implying a momentum transfer and hence a bias in the measurement of the invariant masses. In particular the non-perturbative exchange of soft gluons ($E_g < \Gamma_W$) may have a large impact on the reconstructed W mass.

Colour reconnection is investigated by comparing the charged particle multiplicity in $WW \to q\bar{q}\,q\bar{q}$ and $WW \to q\bar{q}\,\ell\nu$ events [90, 91]. As models predicting extreme effects from colour reconnection are ruled out, the models [92] consistent with the data still result in shifts between 25 MeV and 70 MeV on the reconstructed W mass.

Obeying Bose-Einstein statistics identical mesons from quark fragmentation tend to occupy the same place in momentum space. Such correlations are

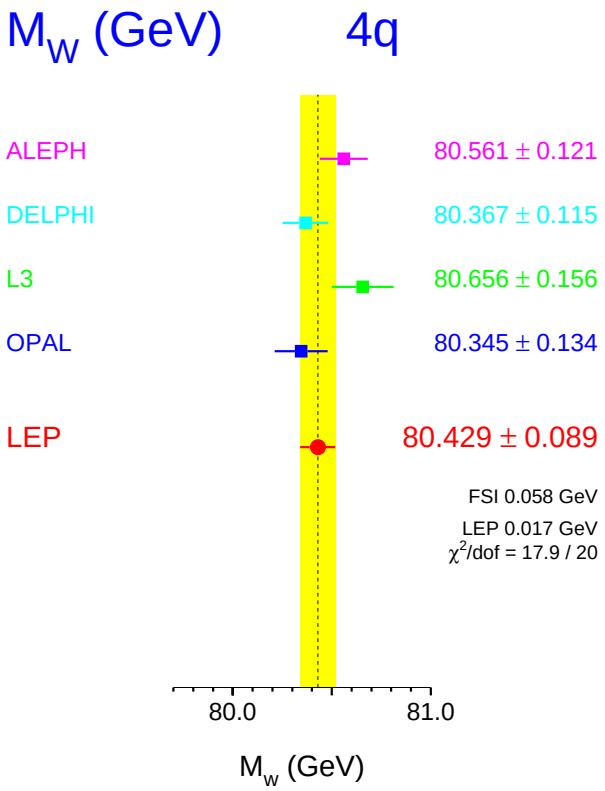

Figure 43. Measurements of the W mass from $WW \to q\bar{q}\,q\bar{q}$ at LEP ($172\ \text{GeV} \le \sqrt{s} \le 189\ \text{GeV}$). Correlated errors from final state interactions and the LEP beam energy calibration are included in the combined result.

experimentally established in hadronic Z and W decays whereas they are not confirmed between mesons stemming from the different W bosons in $e^+e^- \to W^+W^-$ [93]. This uncertainty on the existence of possible correlations between mesons from different W bosons, together with the imperfections in their modelling, may lead to a bias in the W mass reconstruction. Estimates for such a bias range from 20 MeV to 60 MeV.

The results of the LEP W mass measurement from direct reconstruction of the decays products are shown in Figs. 43 and 44 [94,95] based on approximately 3500 $e^+e^- \to W^+W^-$ events per experiment ($172\ \text{GeV} \le \sqrt{s} \le 189\ \text{GeV}$). The combinations of the four experiments yield 80.313 ± 0.063 GeV for $q\bar{q}\,\ell\nu$ and 80.429 ± 0.089 GeV for $q\bar{q}\,q\bar{q}$ final states, the latter containing a contribution to the error from final state interference effects of ± 0.058 GeV. Combining all results obtained by the LEP experiments from the data taken above the WW threshold yields a value for the W mass of:

$$m_W = 80.350 \pm 0.056\ \text{GeV}\,. \qquad (22)$$

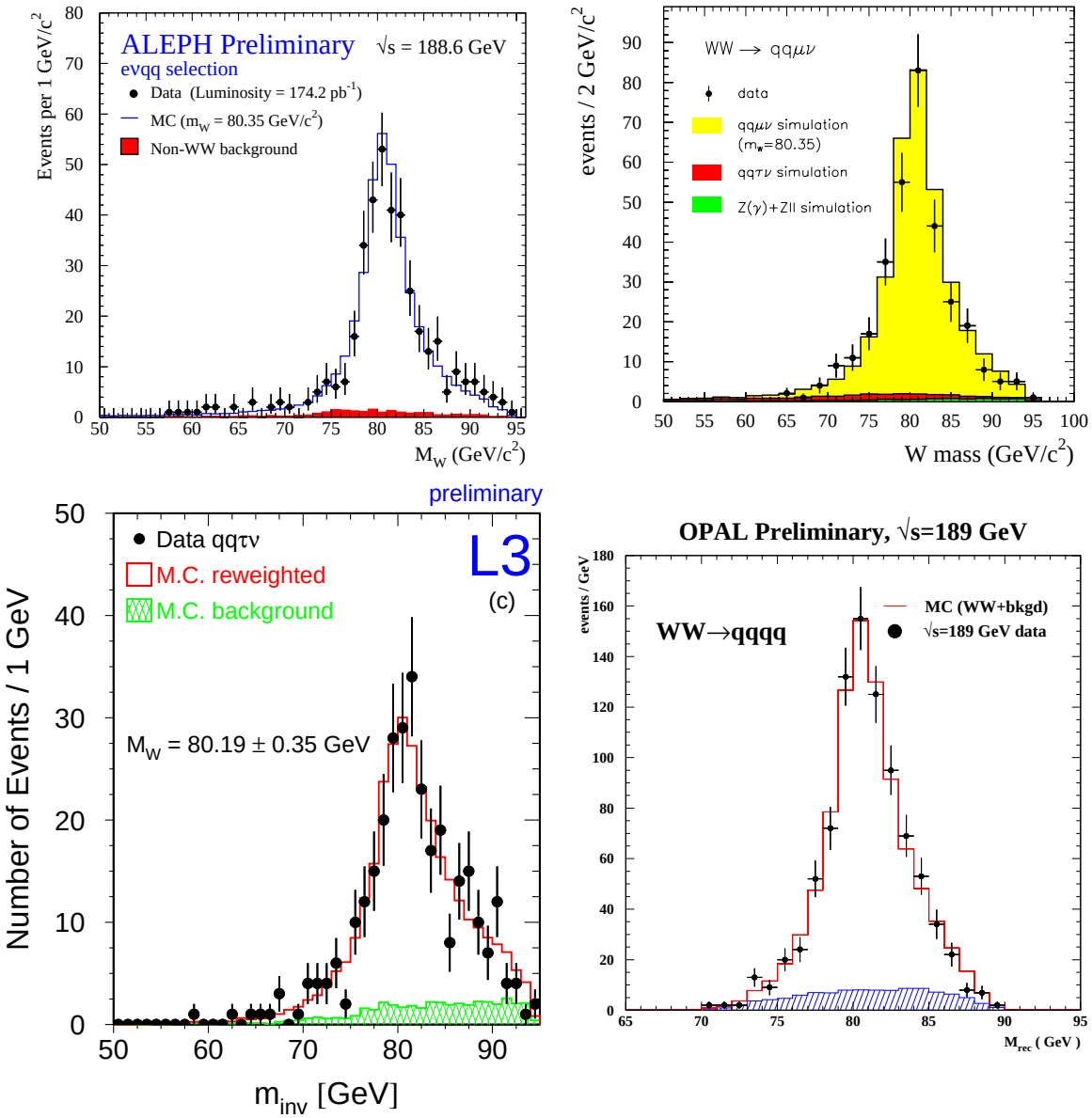

Figure 42. Invariant mass distributions after kinematic fit measured by the LEP experiments at $\sqrt{s} = 189$ GeV. Shown are representative distributions from the four final states used for the W mass measurement: $\mathrm{WW} \to \mathrm{q\bar{q}\,e\nu}$ (ALEPH), $\mathrm{WW} \to \mathrm{q\bar{q}}\,\mu\nu$ (DELPHI), $\mathrm{WW} \to \mathrm{q\bar{q}}\,\tau\nu$ (L3) and $\mathrm{WW} \to \mathrm{q\bar{q}\,q\bar{q}}$ (OPAL).

This includes the W mass measurement obtained from the cross section measurement at the threshold [96].

5.6. Measurement of the W mass at the Tevatron

Precise measurements of the W mass are also performed by the experiments at the Tevatron. New results are available from both experiments which are based on the complete event sample collected in Run I which took place between 1988 and 1995. About 45000 $\mathrm{W} \to \ell\nu$ ($\ell = \mathrm{e}, \mu$) events are used by each collaboration for the m_{W} measurement which is derived from fits to the measured transverse mass and momentum distributions.

The absolute scale of the W mass is determined from the observed leptonic Z boson decays. The measured Z mass is compared to the precise LEP measurement (Tab. 1). Fig. 45 shows the invariant mass distribution in $\mathrm{Z} \to \mu^+\mu^-$ events measured by CDF. The uncertainties in the determination of the absolute

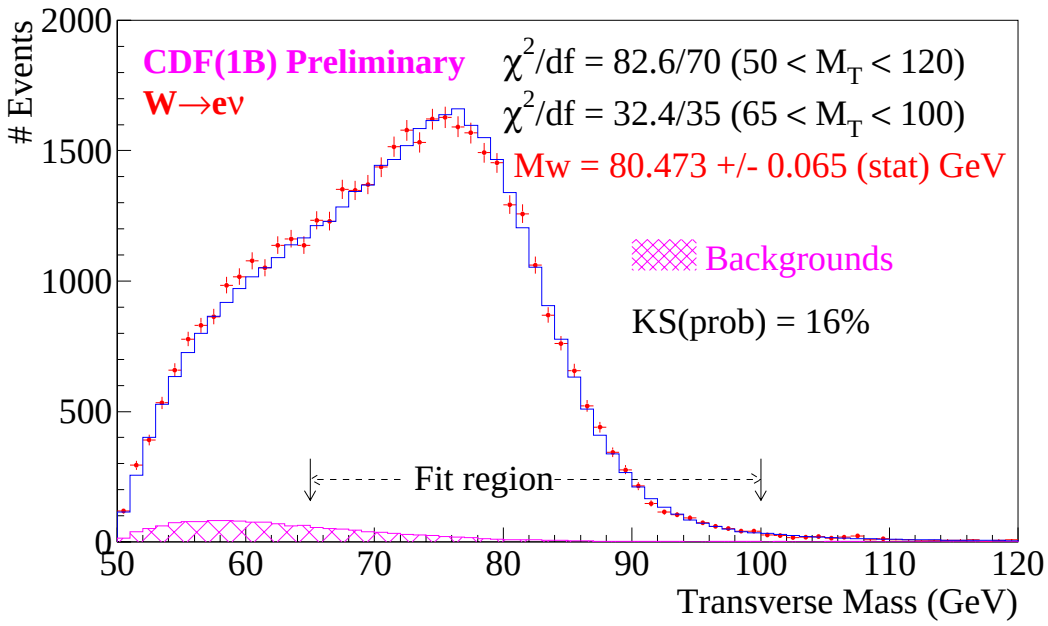

Figure 46. Transverse mass distribution in W $\rightarrow$ eν events as measured by CDF.

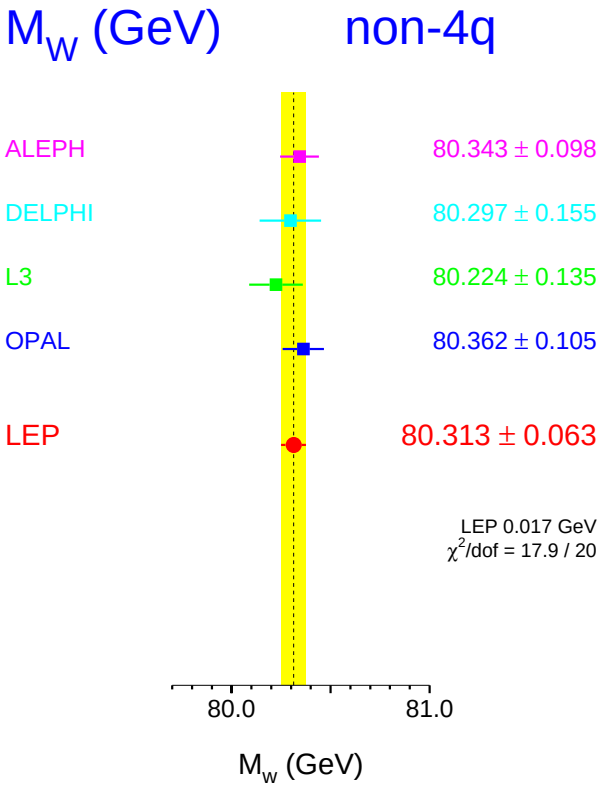

Figure 44. Same as Fig. 43 for WW $\rightarrow$ q$\bar{\text{q}}$ $\ell\nu$.

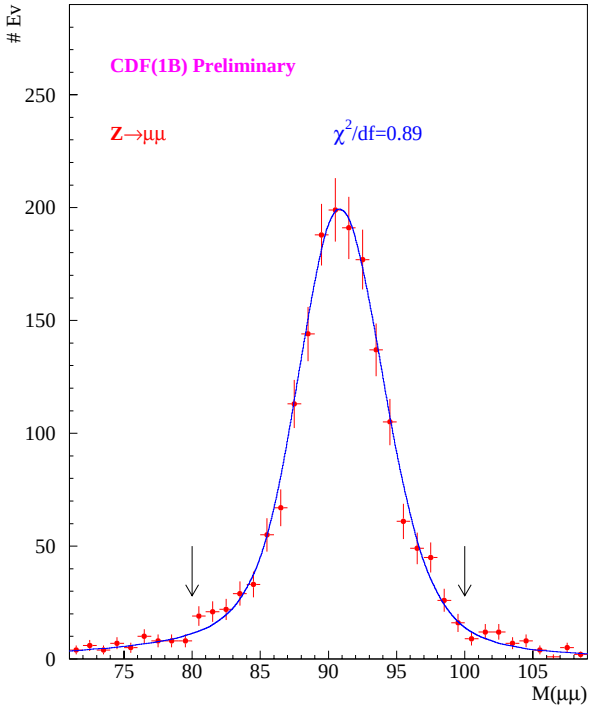

Figure 45. Invariant mass distribution for Z $\rightarrow$ $\mu^+\mu^-$ candidates observed by CDF.

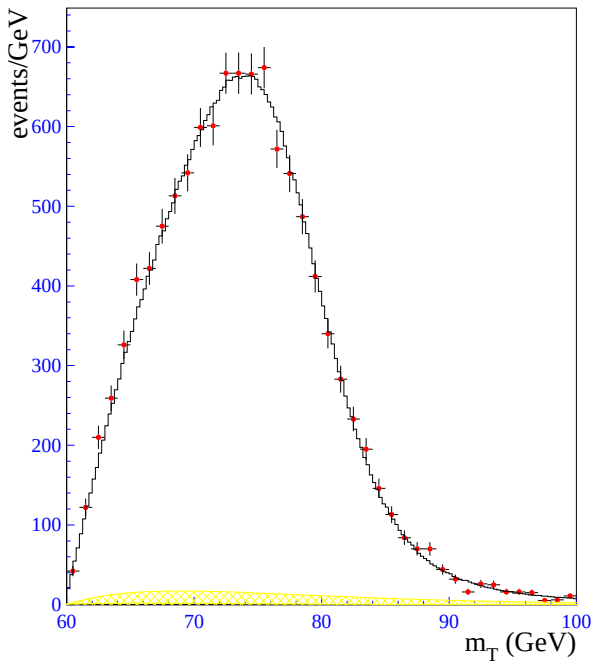

Figure 47. Transverse mass distribution in $W \to e\nu$ events as measured by DØ in the pseudo-rapidity region $1.5 < |\eta| < 2.5$.

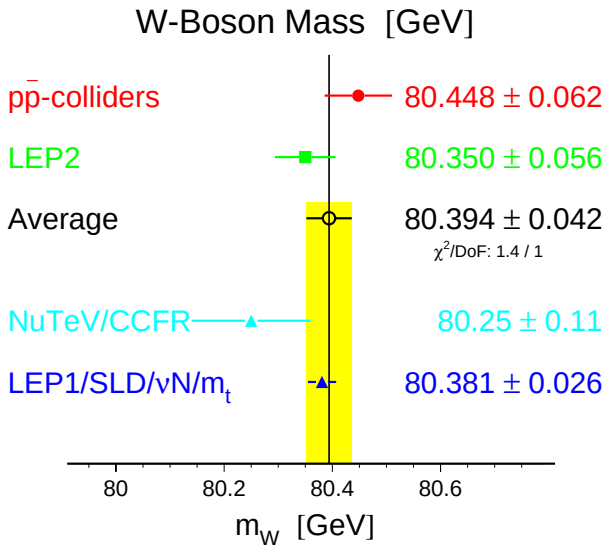

Figure 48. Comparison of W mass measurements. The direct measurements at $p\bar{p}$ colliders and at LEP are averaged and compared to indirect determinations.

energy and momentum scales caused by the limited Z statistics constitute the largest sources of systematic errors on the W mass measurements contributing with ± 75 MeV ($W \to e\nu$) and ± 85 MeV ($W \to \mu\nu$) to the CDF results and with ± 59 MeV to the DØ result.

The main improvement of the CDF measurement as compared to last year is due to the inclusion of the complete electron data set. The measured transverse mass distribution in $W \to e\nu$ events is presented in Fig. 46. Combining these data with the muon channel and with previous data a value of 80.433 ± 0.079 GeV for the W mass is obtained by CDF [97].

The DØ collaboration has now added a measurement of m_W using events in the forward calorimeters of the detector. Fig. 47 shows the transverse mass distribution in the pseudo-rapidity region $1.5 < |\eta| < 2.5$. Combined with the measurement performed in the central detector [98, 99] DØ measures the W mass to be $m_W = 80.474 \pm 0.093$ GeV†.

Assuming a common systematic error of 25 MeV, essentially due to model uncertainties, yields a combined result for the W mass measured at $p\bar{p}$-colliders of [97]:

$$m_W = 80.448 \pm 0.062 \text{ GeV} . \qquad (23)$$

† This result presented at the conference is used below. It differs slightly from the value $m_W = 80.482 \pm 0.091$ GeV published recently [99].

This number contains also the measurement performed by the UA2 experiment [100].

A comparison of different determinations of the W mass is shown in Fig. 48. The direct determinations of m_W in $p\bar{p}$ and e^+e^- collisons are in good agreement and their combination results in a precise measurement of m_W:

$$m_W = 80.394 \pm 0.042 \text{ GeV} . \qquad (24)$$

This value agrees with the indirect determination of m_W obtained from measurements of the weak mixing angle $\sin^2\vartheta_W = 1 - m_W^2/m_Z^2$ in neutrino-nucleon scattering by the NuTeV experiment [101,102] and with the precise value of m_W derived from the measurements at the Z resonance which will be discussed in Sec. 6.

5.7. Measurement of the W width

When determining the W mass from the measured invariant mass distributions (Fig. 42) the total width Γ_W is fixed to the SM prediction. Leaving this parameter free in the fit Γ_W can be determined in a direct way at LEP. Fig. 49 shows the contours in the Γ_W-m_W plane obtained from such a fit using L3 data up to $\sqrt{s} = 189$ GeV. Direct measurements of Γ_W obtained this way at LEP are summarized in Tab. 11 and they are found to be in good agreement with the SM.

At the Tevatron the W width is extracted from the transverse mass distribution in a similar manner. In particular the high end of the spectrum is sensitive to Γ_W. Fig. 50 shows contours obtained from a simultaneous fit to m_W and Γ_W. Combining electron

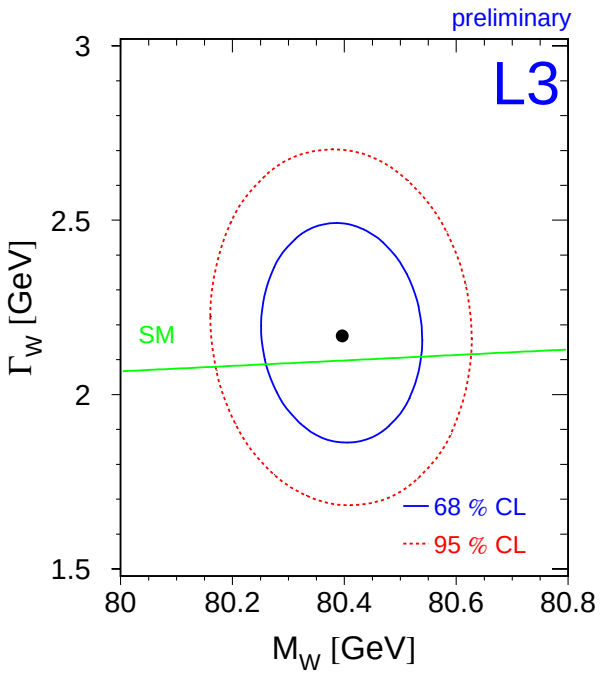

Figure 49. Result of the simultaneous determination of the W mass and width from L3. The central value (dot) and contours obtained from fits to the data are compared to the SM relation (solid line).

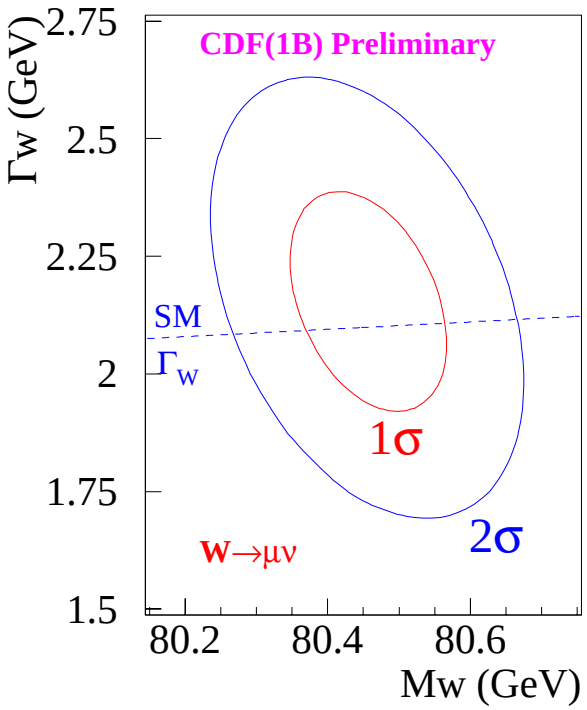

Figure 50. Contours in the $\Gamma_{\rm W} - m_{\rm W}$ plane obtained by CDF from fits to the transverse mass distributions of $\rm W \to \mu\nu$ events.

	$\Gamma_{\rm W}$[GeV]
DELPHI*	2.48 ± 0.41
L3	2.12 ± 0.25
OPAL*	1.84 ± 0.38
SM	2.08

* 183 GeV data only

Table 11. Determinations of the total width of the W at LEP compared to the SM expectation.

and muon data CDF determines the width of the W boson to be [62]:

$$\Gamma_{\rm W} = 2.055 \pm 0.125 \ {\rm GeV} \, . \qquad (25)$$

A much less direct way of determining $\Gamma_{\rm W}$ is provided by the measurement of the ratio of cross sections times leptonic branching fractions of W and Z bosons at the Tevatron. The W width is extracted using SM calculations and LEP measurements:

$$\frac{\sigma(\rm p\bar{p} \to W + X)\, BR(W \to \ell\nu)}{\sigma(\rm p\bar{p} \to Z + X)\, BR(W \to \ell\ell)} = \left(\frac{\sigma_{\rm W}}{\sigma_{\rm Z}}\right)^{\rm SM} \left(\frac{\Gamma_{\rm Z}}{\Gamma_{\rm Z\to\ell\ell}}\right)^{\rm LEP} \frac{\Gamma^{\rm SM}_{\rm W\to\ell\nu}}{\Gamma_{\rm W}} \, . \qquad (26)$$

Many experimental and theoretical uncertainties cancel in these ratios providing the currently most precise results for the W width [62, 103]:

$$\begin{aligned} \Gamma_{\rm W} &= 2.179 \pm 0.046 \ {\rm GeV} \qquad ({\rm CDF}) \, , \\ \Gamma_{\rm W} &= 2.107 \pm 0.054 \ {\rm GeV} \qquad ({\rm D\O}) \, . \end{aligned} \qquad (27)$$

These values are in agreement with the direct measurements of $\Gamma_{\rm W}$ and the SM prediction quoted above.

6. Interpretation of the electroweak measurements in the SM

6.1. The QED coupling constant at the Z

For the calculation of observables at the Z resonance the precise knowledge of the QED coupling constant α at the Z is required. Whereas the contribution to the running of α from its precise definition at low momentum transfer to the Z from charged leptons has been calculated to $\mathcal{O}(\alpha^3)$ [104], the contribution from the five light quark flavours has a relative uncertainty of about 2% [105]:

$$\Delta\alpha^{(5)}_{\rm had} = 0.02804 \pm 0.00065 \, . \qquad (28)$$

This value, derived from an analysis of measurements of the cross section $\rm e^+e^- \to$ hadrons below the Z

resonance, limits the precision of SM calculations and therefore the interpretation of the experimental results, see for instance Fig. 9. It should be noted that smaller errors on $\Delta\alpha^{(5)}_{\rm had}$ are achieved in more theory dependent analyses of the cross section $\mathrm{e^+e^-} \to \mathrm{hadrons}$ at low energies as for example in reference [106].

The BES experiment [107] is measuring the hadronic cross section in the energy range $2\ \mathrm{GeV} \leq \sqrt{s} \leq 5\ \mathrm{GeV}$ which at the moment constitutes the dominant contribution to the uncertainty on α. An energy scan with 85 points has been performed with the aim of measuring cross sections at the percent level and to investigate structures near the charm threshold. First results will be available soon and should allow for a more precise determination of $\Delta\alpha^{(5)}_{\rm had}$ from experimental data.

New cross section measurements of $\mathrm{e^+e^-} \to \pi^+\pi^-$ around the ρ-meson are performed by the CMD-2 experiment [108] providing a significant improvement for the interpretation of the ongoing muon $g-2$ experiment [109].

6.2. Fits in the SM framework

All measurements are consistent with the SM. More profound tests of the theory are achieved by performing fits in the SM framework to all experimental results. The programs ZFITTER and TOPAZ0 are employed in which the calculation of observables is performed within the SM based on five input variables which are the free parameters of these fits: the masses of the Z and Higgs bosons and the top quark, the QED and the strong coupling constants at the Z.

Top quark and Higgs boson masses enter into SM relations through weak radiative corrections [110]. Corrections to the $\mathrm{W}^\pm$ and Z propagators arise from the large mass difference in the third quark doublet which breaks the isospin symmetry and from Higgs boson loops. As a consequence, observables at the Z resonance depend, in first approximation, quadratically on the top quark mass and on the logarithm of the Higgs mass. The QED coupling constant is derived based on $\Delta\alpha^{(5)}_{\rm had}$ which is constrained to the value given in Eq. 28.

The measurements used in the fits are listed in Fig. 51. In addition to the experimental results discussed above the combined result [82, 111] of the direct measurements of the top quark mass performed by the Tevatron experiments [112, 113] is used. Changes and improvements of these measurements as compared to the status of last year are summarized in Fig. 52. Most significant are the improvements in b- and c-quark measurements at the Z resonance, the hadronic Z pole cross section and the W mass measurements at LEP and the Tevatron.

In Tab. 12 the results on the top quark and Higgs boson masses and the strong coupling constant $\alpha_{\rm s}$ at the Z from SM fits to subsets and to all measurements are listed. For the Higgs mass also the logarithm is quoted. From these fit parameters the effective weak mixing angle $\sin^2\overline{\vartheta}_{\rm W}$, its on-shell definition $\sin^2\vartheta_{\rm W}$ and the W boson mass are derived. The results of the fits are in agreement proving the consistency of the measurements and the SM.

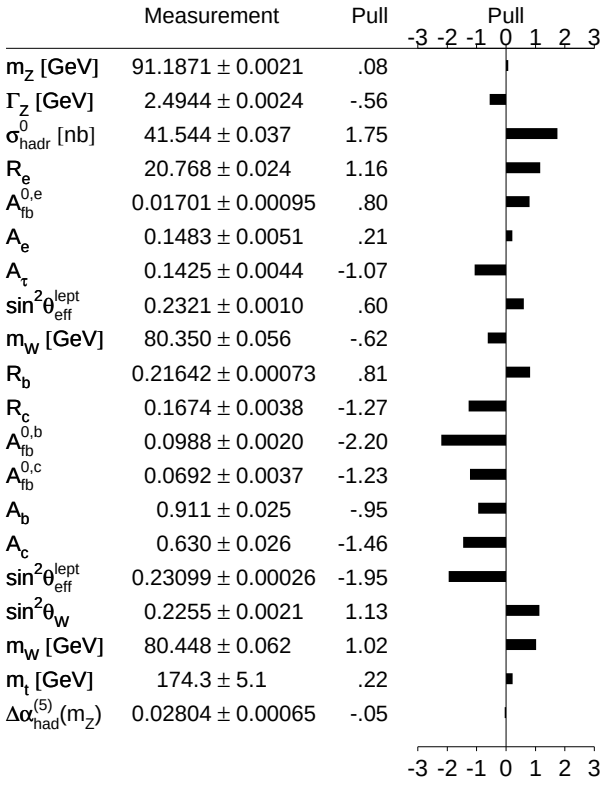

Figure 51. List of measurements used for the fits in the SM framework. Correlations among the LEP Z lineshape measurements and the combined LEP/SLD b- and c-quark measurements are taken into account in the fits. On the right hand side the differences of the measurements with respect to the fit result using all data (Tab. 12) normalized to the error are given.

6.3. Test of the SM model

A particularly illustrative way to test the SM is provided by the comparison of direct and indirect mass measurements. Fig. 53 shows that the direct measurements of the W boson and top quark masses at LEP and the Tevatron are in perfect agreement with the result of the SM fit to all other electroweak measurements.

The equality of the two W mass results is an experimental confirmation of one of the cornerstones

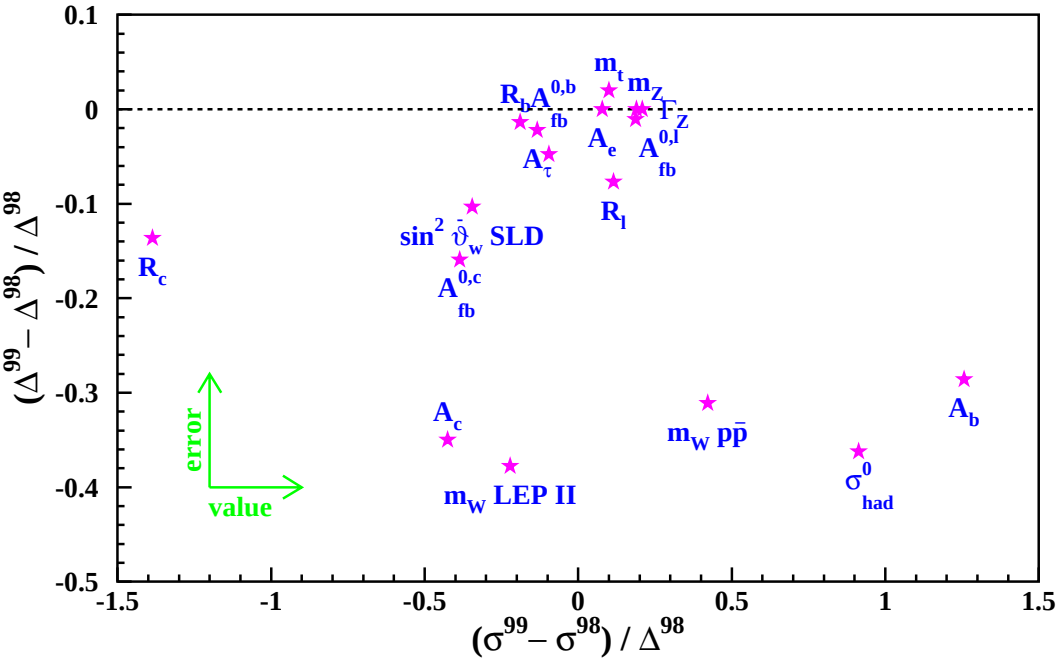

Figure 52. Changes and improvements of measurements used for the fits in the SM framework as compared to summer 1998 [18, 20]. Shown is the difference in the error (Δ) versus the difference in central value (σ), both normalized to the error of the measurement in 1998. Parameters with relative changes of less than 0.05 are suppressed.

	LEP including LEP II m_W	all data except m_W and m_t	all data except m_W	all data
m_t [GeV]	172^{+14}_{-11}	167^{+11}_{-8}	172.9 ± 4.7	173.2 ± 4.5
m_H [GeV]	134^{+268}_{-81}	55^{+84}_{-27}	81^{+77}_{-42}	77^{+69}_{-39}
$\log(m_H/\mathrm{GeV})$	$2.13^{+0.48}_{-0.40}$	$1.74^{+0.40}_{-0.30}$	$1.91^{+0.29}_{-0.32}$	$1.88^{+0.28}_{-0.30}$
α_s	0.120 ± 0.003	0.118 ± 0.003	0.119 ± 0.003	0.118 ± 0.003
χ^2/d.o.f.	$11/9$	$21/12$	$21/13$	$23/15$
$\sin^2\overline{\vartheta}_W$	0.23184 ± 0.00021	0.23151 ± 0.00017	0.23152 ± 0.00017	0.23150 ± 0.00016
$\sin^2\vartheta_W$	0.2237 ± 0.0006	0.2233 ± 0.0007	0.2230 ± 0.0005	0.2229 ± 0.0004
m_W [GeV]	80.342 ± 0.032	80.366 ± 0.035	80.381 ± 0.026	80.385 ± 0.022

Table 12. Results of fits in the SM framework. Four fits are performed using different subsets of the measurements given in Fig. 51. In all cases the constraint on the QED coupling constant (Eq. 28) is used.

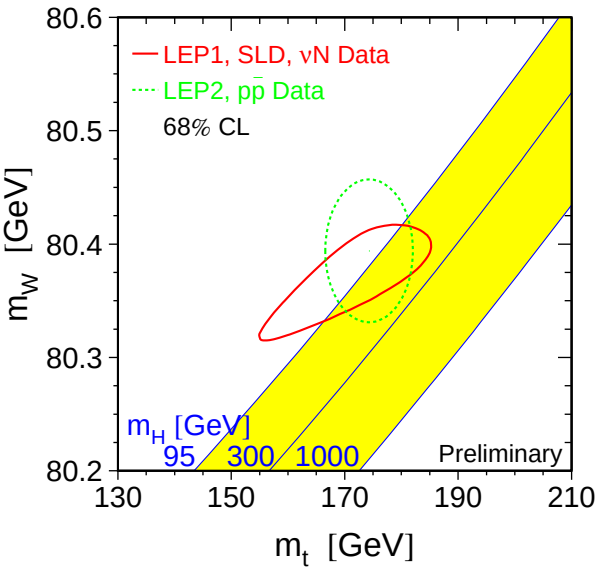

Figure 53. Comparison of direct (dashed contour) and indirect (solid) determinations of the W boson and top quark masses. The solid lines show the SM model relation for three different Higgs boson masses.

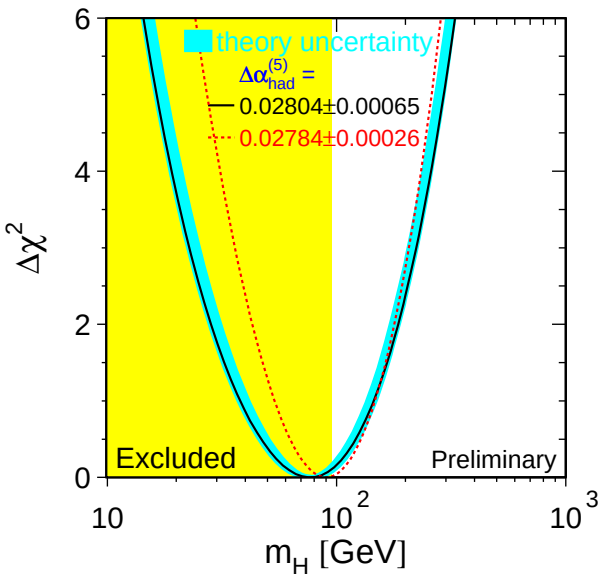

Figure 54. Result of the SM fit to all electroweak precision data. The solid line with band shows the dependence of the χ^2 on the Higgs mass with the estimated theoretical error on the calculation. The dashed line represents the result of the fit using the determination of $\Delta\alpha^{(5)}_{\rm had}$ of reference [106]. The shaded region at the left is excluded by the search for Higgs boson production at LEP (Eq. 31).

of the SM, namely the double role of the heavy gauge bosons as observable particles with masses determining electroweak couplings. Equivalently, the ratio of the W masses derived from the two approaches consist a measurement of the ρ-parameter which, apart from higher order corrections, is unity in the minimal SM with one Higgs doublet [114].

In addition the agreement of the directly measured top quark mass with the value inferred from electroweak observables confirms the existence of weak radiative corrections. Their magnitude is as predicted by the SM showing that the theory is correct beyond the tree level. This non-trivial result is encouraging to go one step further and try to determine the mass of the Higgs boson in a similar way from its contribution to the weak radiative corrections.

6.4. The mass of the Higgs boson

Also shown in Fig. 53 is the SM relation between top and W masses for different values of $m_{\rm H}$. Both contours point consistently to a low value for the Higgs mass. Using all measurements together the mass of the SM Higgs boson is determined to be:

$$m_{\rm H} = 77^{+69}_{-39}\ {\rm GeV}\,. \qquad (29)$$

The dependence of the χ^2 of this fit on $m_{\rm H}$ is shown in Fig. 54. From this curve an upper limit on the Higgs mass is derived:

$$m_{\rm H} < 215\ {\rm GeV} \qquad 95\%\ {\rm CL}\,. \qquad (30)$$

The calculation is repeated using the evaluation of $\Delta\alpha^{(5)}_{\rm had}$ of reference [106] which illustrates the gain in precision on $m_{\rm H}$ which could be obtained from an improved determination of this quantity.

The production of Higgs bosons at LEP is searched for by the experiments. No evidence is found so far in the data up to $\sqrt{s} \leq 189$ GeV which translates into a lower limit on the mass of [35]:

$$m_{\rm H} > 95.2\ {\rm GeV} \qquad 95\%\ {\rm CL}\,. \qquad (31)$$

The search for the Higgs boson together with the limit obtained from electroweak measurements are now severely constraining the allowed mass range. If it exists this last unobserved particle of the SM could be in the reach of the LEP experiments.

7. Summary and outlook

The LEP and SLD experiments are completing one decade of precision physics at the Z. Plenty of experimental results are available which confirm the SM of electroweak interactions to high accuracy. The measurements which have been performed at the Z exceed the expectations and will remain unchallenged for many years.

LEP is now in the middle of the second phase of its scientific program operating at cms energies above the W-pair threshold. Many aspects of the SM like electroweak unification and self couplings of the gauge bosons are investigated.

Rapid progress has been made in the determination of properties of the W boson at LEP and the Tevatron. The most prominent example is the direct measurement of the W boson mass with a combined result of $m_{\mathrm{W}} = 80.394 \pm 0.042$ GeV.

So far all experimental results can be accommodated for in the SM and there is compelling evidence that the Higgs boson is light.

LEP will continue to run until the end of the year 2000. The number of $\mathrm{e^+e^-} \to \mathrm{W^+W^-}$ events collected by the detectors will approximately be doubled leading to significant improvements in the determination of W properties. The accelerator has meanwhile attained $\sqrt{s} = 202$ GeV and there are good prospects for a further increase in energy. This will allow the experiments to enlarge the discovery range for the Higgs boson to $m_{\mathrm{H}} \approx 110$ GeV. The indirect determination of m_{H} from electroweak precision data will profit, in addition to new results on m_{W}, from the anticipated improvements on $\Delta\alpha^{(5)}_{\mathrm{had}}$ from measurements of the hadron cross section at low energy.

The Tevatron collider will start the high luminosity Run II in the year 2000. Further improvements on the W boson and top quark masses are expected. In the case it is too heavy to be seen at LEP the Tevatron experiments may take over the baton in the search for the Higgs boson [115].

8. Acknowledgements

I would like to thank my colleagues from the LEP, SLD and Tevatron experiments and from theory for providing preliminary results of their work for this presentation. Particular thanks are due to the members of the LEP Electroweak Working Group for the combination of many results in a very short time. Also, I am grateful to R. Clare, M. Grünewald and M. Pohl for the careful reading of the manuscript and their valuable suggestions.

References

[1] S.L. Glashow, Nucl. Phys. **22** (1961) 579; S. Weinberg, Phys. Rev. Lett. **19** (1967) 1264; A. Salam, "Elementary Particle Theory", Ed. N. Svartholm, (Almqvist and Wiksell, Stockholm, 1968), 367.

[2] G. Quast, "Electroweak Review at LEP1", these proceedings.

[3] L3 Collab., contributed paper #6_259; OPAL Collab., contributed paper #6_81. Contributed papers of the LEP experiments are available from http://alephwww.cern.ch/ALPUB/conf/conf.html, http://delphiwww.cern.ch/ pubxx/delwww/www/delsec/conferences/tampere99/, http://l3www.cern.ch/conferences/EPS99/, http://www1.cern.ch/Opal/pubs/eps99_sub.html.

[4] ALEPH Collab., R. Barate et al., "Measurement of the Z Resonance Parameters at LEP", Preprint CERN-EP/99-104, CERN, 1999, submitted to E. Phys. J. C.

[5] D. Bardin et al., "A Semi-Analytical Program for Fermion-Pair Production in $\mathrm{e^+e^-}$ Annihilation", Preprint DESY 99-070; P. Christova, M. Jack and T. Riemann, "Hard Photon Emission in $\mathrm{e^+e^-} \to \bar{\mathrm{f}}\mathrm{f}$ with Realistic Cuts", Preprint DESY 99-015, hep-ph/9902408, submitted to Phys. Lett. B.

[6] G. Montagna et al., Nucl. Phys. **B 401** (1993) 3; Comp. Phys. Comm. **76** (1993) 328.

[7] W. Beenaker, F.B. Berends and S.C. van der Marck, Nucl. Phys. **B 349** (1991) 323.

[8] S. Jadach et al., Phys. Lett. **B 257** (1991) 173; M. Skrzypek, Acta Phys. Pol. **B 23** (1992) 135; G. Montagna et al., Phys. Lett. **B 406** (1997) 243.

[9] G. Degrassi et al., Phys. Lett. **B 383** (1996) 219; Phys. Lett. **B 394** (1997) 188; Phys. Lett. **B 418** (1997) 209.

[10] S. Larin et al., Phys. Lett. **B 400** (1997) 379; Phys. Lett. **B 405** (1997) 327; K.G. Chetyrkin et al., Phys. Rev. Lett. **79** (1997) 2184; Nucl. Phys. **B 510** (1998) 61.

[11] A. Czarnecki et al., Phys. Rev. Lett. **77** (1996) 3955; R. Harlander et al., Phys. Lett. **B 426** (1998) 125.

[12] "Reports of the Working Group on Precision Calculations for the Z Resonance", eds. D. Bardin, W. Hollik and G. Passarino, CERN Report CERN 95-03 (1995).

[13] D. Bardin, M. Grünewald and G. Passarino, "Precision Calculation Project Report", Preprint hep-ph/9902452.

[14] A. Arbuzov, "Light pair corrections to electron-positron annihilation at LEP/SLC", Preprint hep-ph/9907500.

[15] The LEP Electroweak Working Group, G. Duckeck et al., "Precise determination of Z-boson parameters from combined results of the LEP experiments", Note available from http://www.cern.ch/LEPEWWG/.

[16] B.F.L Ward et al., Phys. Lett. **B 450** (1999) 262.

[17] M. Consoli et al. in "Z Physics at LEP I", CERN Report CERN 89-08 (1989), Vol. 1, p. 7, eds. G. Altarelli, R. Kleiss and C. Verzegnassi.

[18] The LEP Experiments ALEPH, DELPHI, L3 and OPAL, the LEP Electroweak Working Group and the SLD Heavy Flavour Group, "A Combination of Preliminary Electroweak Measurements and Constraints on the Standard Model", Preprint CERN-EP/99-015, CERN, 1999.

[19] Working Group on LEP Energy, R. Assmann et al., E. Phys. J. **C 6** (1999) 187.

[20] D. Karlen, "Experimental status of the Standard Model", presentation at the ICHEP 98 conference, Vancouver (1998), to appear in the proceedings.

[21] J.E. Brau, "Electroweak Precision Measurements with Leptons", these proceedings.

[22] J. Mnich, Phys. Rep. **271** (1996) 181.

[23] The LEP Experiments ALEPH, DELPHI, L3 and OPAL, Nucl. Inst. Meth. **A 378** (1996) 101.

[24] The LEP/SLD Heavy Flavour Working Group, D. Abbaneo et al., "Heavy Flavour Results presented at the 1999 Winter Conferences", Note available from http://www.cern.ch/LEPEWWG/heavy/.

[25] S. Fahey, "Quark Coupling at the Z", these proceedings.

[26] SLD Collab., contributed paper #6_165.

[27] DELPHI Collab., contributed paper #6_211.

[28] ALEPH Collab., contributed paper #1_392; DELPHI Collab., contributed papers #6_365 and #6_369; L3 Collab., contributed paper #1_232; OPAL Collab., contributed paper #1_80.

[29] ALEPH Collab., contributed paper #6_694; DELPHI Collab., contributed paper #6_362; L3 Collab., contributed paper #6_262.

[30] ALEPH Collab., R. Barate et al., "Study of Fermion pair production in $\mathrm{e^+e^-}$ collisions at 130-183 GeV", Preprint CERN-EP/99-042, CERN, 1999, submitted to E. Phys. J. C; OPAL Collab., G. Abbiendi et al., "Tests of the Standard Model and Constraints on New Physics from Measurements of Fermion-pair Production at 189 GeV at LEP", Preprint CERN-EP/99-097, CERN, 1999, submitted to E. Phys. J. C.

[31] The LEP Electroweak Working Group, D. Bourilkov et al., "Combination of the LEP2 $\mathrm{f\bar{f}}$ Results", Note available from http://www.cern.ch/LEPEWWG/.

[32] M. Minard, "Fermion-pair Production at LEP2 from 130 to 196 GeV", these proceedings.

[33] E. Eichten, K. Lane and M. Peskin, Phys. Rev. Lett. **50** (1983) 81.

[34] H. Rick, "Tests of the Validity of the Standard Model", these proceedings.

[35] E. Gross, "Searches for New Particles", these proceedings.

[36] ALEPH Collab., contributed paper #6_429; DELPHI Collab., contributed paper #6_141; OPAL Collab., contributed paper #62.

[37] L3 Collab., M. Acciarri et al., "Single and Multi-Photon Events with Missing Energy in $\mathrm{e^+e^-}$ Collisions at $\sqrt{s} = 189$ GeV", Preprint CERN-EP/99-129, CERN, 1999, submitted to Phys. Lett. B.

[38] "The 1998 Review of Particle Physics", C. Caso et al, E. Phys. J. **C 3** (1998) 1.

[39] L3 Collab., M. Acciarri et al., Phys. Lett. **B 431** (1998) 387.

[40] ALEPH Collab., contributed paper #6_694; DELPHI Collab., contributed paper #6_219; L3 Collab., contributed paper #6_283; OPAL Collab., contributed paper #21.

[41] E. Elsen, "Tests of the SM in Inclusive Hard Scattering at HERA", these proceedings.

[42] ALEPH Collab., contributed paper #6_429; DELPHI Collab., contributed paper #6_364; L3 Collab., contributed paper #6_251.

[43] OPAL Collab., G. Abbiendi et al., "Multi-photon production in $\mathrm{e^+e^-}$ collisions at $\sqrt{s} = 189$ GeV", Preprint CERN-EP/99-088, CERN, 1999, submitted to Phys. Lett. B.

[44] L3 Collab., M. Acciarri et al., Phys. Lett. **B 439** (1998) 183; L3 Collab., contributed paper #6_266.

[45] OPAL Collab., contributed paper #16.

[46] L3 Collab., M. Acciarri et al., Phys. Lett. **B 450** (1999) 281.

[47] L3 Collab., M. Acciarri et al., "Study of Z Boson Pair Production in $\mathrm{e^+e^-}$ Collisions at LEP at $\sqrt{s} = 189$ GeV", Preprint CERN-EP/99-119, CERN, 1999, submitted to Phys. Lett. B.

[48] ALEPH Collab., contributed paper #6_398; DELPHI Collab., contributed paper #6_430; OPAL Collab., contributed paper #64.

[49] E. Sánchez, "ZZ Production at LEP", these proceedings.

[50] K. Hagiwara et al., Nucl. Phys. **B 282** (1987) 253.

[51] DELPHI Collab., contributed paper #6_249; L3 Collab., contributed paper #6_250.

[52] DØ Collab., B. Abott et al., Phys. Rev. **D 57** (1998) 3817.

[53] U. Baur and E. Berger, Phys. Rev. **D 47** (1993) 4889.

[54] A. Barzcyk, "W boson properties at LEP", these proceedings.

[55] ALEPH Collab., R. Barate et al., Phys. Lett. **B 453** (1999) 107; DELPHI Collab., P. Abreu et al., Phys. Lett. **B 456** (1999) 310; L3 Collab., M. Acciarri et al., Phys. Lett. **B 436** (1998) 437.

[56] M. Skrzypek et al., Comp. Phys. Comm. **94** (1996) 216; Phys. Lett. **B 372** (1996) 289.

[57] ALEPH Collab., contributed paper #6_405; DELPHI Collab., contributed paper #6_78; L3 Collab., contributed paper #6_253; OPAL Collab., contributed paper #6_60.

[58] A. Ballestrero, " LEP2 four-fermion review", these proceedings.

[59] W. Beenaker et al., in "Physics at LEP 2", Report CERN 96-01 (1996), eds. G. Altarelli, T. Sjöstrand, F. Zwirner, Vol. 1, p. 79.

[60] ALEPH Collab., R. Barate et al., "A direct measurement of $|V_{\rm cs}|$ in hadronic W decays using a charm tag", Preprint CERN-EP/99-124, CERN, 1999, submitted to Phys. Lett. B.

[61] OPAL Collab., contributed paper #5_61.

[62] J. Ellison, "W and Z properties at the Tevatron", these proceedings.

[63] ALEPH Collab., contributed paper #5_621; DELPHI Collab., contributed paper #5_107.

[64] OPAL Collab., G. Abbiendi et al., Phys. Lett. **B 447** (1999) 134.

[65] DELPHI Collab., contributed paper #5_715; L3 Collab., contributed paper #6_287;.

[66] I. Boiko, "Tests of lepton universality in tau decays", these proceedings.

[67] S. Gentile and M. Pohl, Phys. Rep. **274** (1996) 287.

[68] G. Gounaris et al., in "Physics at LEP 2", Report CERN 96-01 (1996), eds. G. Altarelli, T. Sjöstrand, F. Zwirner, Vol. 1, p. 525.

[69] ALEPH Collab., contributed paper #6_399; DELPHI Collab., contributed paper #6_360; L3 Collab., contributed paper #6_254; OPAL Collab., contributed paper #10.

[70] A. Macchiolo, "Triple Gauge Couplings in $\rm W^+W^-$ events at LEP", these proceedings.

[71] DELPHI Collab., P. Abreu et al., Phys. Lett. **B 459** (1999) 382; L3 Collab., M. Acciarri et al., "Measurement of Triple-Gauge-Boson Couplings of the W Boson at LEP", Preprint CERN-EP/99-131, CERN, 1999, submitted to Phys. Lett. B; OPAL Collab., G. Abbiendi et al., E. Phys. J. **C 8** (1999) 191.

[72] DØ Collab., B. Abbott et al., "Studies of WW and WZ Production and Limits on Anomalous $\rm WW\gamma$ and WWZ Couplings", Preprint Fermilab-Pub-99/139-E, Fermilab, 1999, submitted to Phys. Rev.

[73] J. Fujimoto et al., Comp. Phys. Comm. **100** (1997) 128.

[74] F. Berends, R. Pittau and R. Kleiss, Comp. Phys. Comm. **85** (1995) 437.

[75] ALEPH Collab., contributed paper #6_427; DELPHI Collab., contributed paper #6_681; L3 Collab., contributed paper #6_256.

[76] O. Yushchenko, "Single-W Production and Neutral TGC at LEP2", these proceedings.

[77] OPAL Collab., G. Abbiendi et al., "Measurement of the $\rm W^+W^-\gamma$ Cross-section and First Direct Limits on Anomalous Electroweak Quartic Gauge Couplings", Preprint CERN-EP/99-130, CERN, 1999, submitted to Phys. Lett. B.

[78] G. Bélanger and F. Boudjema, Phys. Lett. **B 288** (1992) 201.

[79] M. Thomson, "$\rm WW\gamma$ Cross Section and First Direct Limits on Anomalous Quartic Gauge Couplings", these proceedings.

[80] O. Eboli, M. Gonzaléz and S. Novaes, Nucl. Phys. **B 411** (1994) 381.

[81] L3 Collab., Note #2441, contributed paper.

[82] P. Koehn, "Results on top quark properties from CDF", these proceedings.

[83] CDF Collab., T. Affolder et al., "Measurement of the Helicity of W Bosons in Top Quark Decays", Preprint FERMILAB PUB-99/257-E, FERMILAB, 1999, submitted to Phys. Rev. Lett.

[84] ALEPH Collab., R. Barate et al., Phys. Lett. **B 453** (1999) 121; DELPHI Collab., P. Abreu et al., "Measurement of the mass of the W boson using direct reconstruction at $\sqrt{s} = 183$ GeV", Preprint CERN-EP/99-079, CERN, 1999, submitted to Phys. Lett. B; L3 Collab., M. Acciarri et al., Phys. Lett. **B 454** (1999) 386; OPAL Collab., G. Abbiendi et al., Phys. Lett. **B 453** (1999) 138.

[85] ALEPH Collab., contributed paper #6_403; DELPHI Collab., contributed paper #6_367; L3 Collab., contributed paper #6_255; OPAL Collab., contributed paper #26.

[86] LEP Polarization Collaboration, L. Arnaudon et al., Phys. Lett. **B 284** (1992) 431.

[87] The LEP Energy Working Group, A. Blondel et al., "Evaluation of the LEP centre-of-mass energy above the W-pair production threshold", Preprint CERN-EP/98-191, CERN, 1998, submitted to E. Phys. J. C.

[88] The LEP Energy Working Group, R. Assmann et al., "Evaluation of the LEP centre-of-mass energy for data taken in 1998", Note available from http://www.cern.ch/LEPECAL/.

[89] E. Torrence, "Determination of the LEP Beam Energy", these proceedings.

[90] ALEPH Collab., contributed paper #1_387; DELPHI Collab., contributed paper #1_229; L3 Collab., contributed paper #1_258.

[91] OPAL Collab., G. Abbiendi et al., Phys. Lett. **B 453** (1999) 153.

[92] T. Sjöstrand and V.A. Khoze, Phys. Rev. Lett. **72** (1994) 28; Z. Phys. **C 62** (1994) 281.

[93] ALEPH Collab., contributed paper #1_388; L3 Collab., contributed paper #1_257; OPAL Collab., contributed paper #29.

[94] R. Chierici, "W Mass from Fully Leptonic and Mixed Decays at LEP", these proceedings.

[95] L. Mir, "W Mass from Fully Hadronic Decays at LEP", these proceedings.

[96] The LEP Experiments ALEPH, DELPHI, L3 and OPAL, the LEP Electroweak Working Group and the SLD Heavy Flavour Group, "A Combination of Preliminary Electroweak Measurements and Constraints on the Standard Model", Preprint CERN-PPE/97-154, CERN, 1997.

[97] B. Carithers, "New W Mass Measurements from CDF/DØ", these proceedings.

[98] DØ Collab., B. Abott et al., Phys. Rev. Lett. **80** (1998) 3008.

[99] DØ Collab., B. Abott et al., "A measurement of the W boson mass using large rapidity electrons", Preprint FERMILAB PUB-99/237-E, FERMILAB, 1999, submitted to Phys. Rev. D.

[100] UA2 Collab., J. Alitti et al., Phys. Lett. **B 276** (1992) 354.

[101] CCFR/NuTeV Collab., K. McFarland et al., E. Phys. J. **C 1** (1998) 509.

[102] K. McFarland, "Measurement $\sin^2\Theta_{\rm W}$ in νN from NuTeV", these proceedings.

[103] DØ Collab., B. Abott et al., "Extraction of the Width of the W Boson from Measurements of $\sigma(\mathrm{p\bar{p}} \to \mathrm{W} + X) \cdot B(\mathrm{W} \to \mathrm{e}\nu)$ and $\sigma(\mathrm{p\bar{p}} \to \mathrm{Z} + X) \cdot B(\mathrm{Z} \to \mathrm{ee})$ and their Ratio", Preprint FERMILAB PUB-99/171-E, FERMILAB, 1999, submitted to Phys. Rev. D.

[104] M. Steinhauser, Phys. Lett. **B 429** (1998) 158.

[105] S. Eidelman and F. Jegerlehner, Z. Phys. **C 67** (1995) 585.

[106] M. Davier and A. Höcker, Phys. Lett. **B 419** (1998) 419.

[107] Y. Zhu, "Measurement of the Total Hadronic Cross Section in the $\sqrt{s} = 2 - 5$ GeV Range at BES", these proceedings.

[108] CMD-2 Collab., R. Akhmetshin et al., "Measurement of $\mathrm{e^+e^-} \to \pi^+\pi^-$ with CMD-2 around ρ-meson", Preprint Budker INP 99-10, Novosibirsk, hep-ex/9904027.

[109] P. Cushman, "Brookhaven Muon $g - 2$ Experiment", these proceedings.

[110] M. Consoli et al. in "Z Physics at LEP I", CERN Report CERN 89-08 (1989), Vol. 1, p. 55, eds. G. Altarelli, R. Kleiss and C. Verzegnassi.

[111] A. Helnson, "Recent Results on the Top Quark from the Tevatron Collider Experiments", presentation at the XXXIV Rencontres de Moriond, Les Arcs (1999), to appear in the proceedings.

[112] CDF Collab., F. Abe et al., Phys. Rev. Lett. **D 80** (1998) 2767; Phys. Rev. Lett. **D 80** (1998) 2779; Preprint FERMILAB PUB-98/319-E, submitted to Phys. Rev. Lett.; Phys. Rev. Lett. **D 82** (1999) 271.

[113] DØ Collab., B. Abott et al., Phys. Rev. Lett. **D 80** (1998) 2063; Phys. Rev. **D 58** 052001 (1998); Phys. Rev. **D 60** 052001 (1999).

[114] M. Veltman, Nucl. Phys. **B 123** (1977) 89; M.S. Chanowitz et al., Phys. Lett. **B 78** (1978) 1; M. Consoli, S. Lo Presti and L. Maiani, Nucl. Phys. **B 223** (1983) 474; J. Fleischer and F. Jegerlehner, Nucl. Phys. **B 228** (1983) 1.

[115] M. Roco, "Higgs Discovery Prospects at the Tevatron", these proceedings.